

**GEOFORSCHUNGSZENTRUM POTSDAM**  
STIFTUNG DES ÖFFENTLICHEN RECHTS

---

# Scientific Technical Report

# **Radioholographic Analysis of Radiooccultation Data**

**Oleg I. Yakovlev, Alexandre G. Pavelyev,  
Stanislav S. Matyugov, Dmitrii A. Pavelyev,  
Vladimir A. Anufriev**

**Institute of Radio Engineering and Electronics  
of the Russian Academy of Sciences, Moscow**

## Table of contents

Abstract	3
Introduction	5
1. Radio holographic method: Main results	7
1.1. Generalization of radio holographic method for three dimensional case	7
1.2. Radio holographic method as generalized form of backward propagation method	9
1.3. Validation of radio holographic method by means of observation of reflected signal in GPS/MET radio occultation data	11
1.4. Comparing vertical resolution of the radio holographic and backward methods	12
1.5. Observation of wave structures in the upper atmosphere by radio holographic method	14
2. Development of method for monitoring of statistical atmospheric and ionospheric irregularities using radio occultation method	17
2.1. Phase fluctuations at $\lambda=19$ cm (GPS/MET experiment )	17
2.2. Amplitude fluctuations at $\lambda=2$ cm (MIR/GEO experiment)	19
Figures	21
Summary	35
Recommendations	37
References	38



## Abstract

The report describes the main results of investigations performed in 2001 year in framework of a research contract between GeoForschungsZentrum Potsdam (GFZ) and the Institute of Radio Engineering and Electronics of the Russian Academy of Sciences, Moscow (IRE).

1. It is shown that the 2-D focused synthetic aperture radiographic method derived earlier by *Pavelyev* [1998], *Hocke et al.* [1999], *Igarashi et al.* [2000, 2001] provides a full solution of the task of the backward propagation approach and gives vertical resolutions of about 60 - 80 m as follows from analysis of radio occultation data. For achieving very high vertical resolution of about 1/20 - 1/100 of the size of the Fresnel zone it is necessary to construct new radio holographic algorithms. These algorithms will use effective solution processes of direct and inverse refraction and the diffraction problem for inhomogeneous media and must work in real time. The validation of the 2-D focused synthetic aperture radiographic method is performed by means of discovering reflected signals in GPS/MET data and measuring parameters of wave structures in the upper atmosphere. The first radio images of the atmosphere and terrestrial surface were obtained using GPS/MET radio occultation data. Radio images may be used for bistatic scatterometry of the terrestrial surface: determination of parameters of the sea surface (for example, estimation of heights and slopes of the wind roughness) and land. Radio images of the atmosphere may also be used for estimating parameters of multibeam propagation and vertical profiles of the refractivity, temperature and humidity in the boundary layer. A model describing the dependence of the phase path, amplitude and frequency of reflected signals on vertical profiles of the refractive index and absorption in the atmosphere is developed. This model may be used for measurements of the refractivity, humidity and absorption in the boundary layer of the atmosphere.
2. An ionospheric correction algorithm is developed. This algorithm excluded the influence of the upper layer of the F-layer for quiet ionosphere conditions. The influence of the ionosphere has been considered as a slow trend, which may be subtracted from the phase data at two frequencies. It is shown that for quiet ionospheric conditions the influence of layered structures near the turning point of a radio occultation ray is about 40 dB greater than the effect of the upper ionosphere irregularities on the radio occultation signal. In the case of high solar activity the influence of the upper ionosphere may be essential especially near an auroral oval and near the geomagnetic equator. In this case amplitude and phase fluctuations of the radio occultation signal caused by the upper ionosphere may be higher than effects of layered structures in the atmosphere and lower ionosphere. Excluding the ionospheric effect in the case of high solar activity is the subject of future work.
3. A new method of monitoring of density and temperature fluctuations in the stratosphere from radio occultation amplitude measurements for satellite-to-satellite links (MIR/GEO) has been introduced. The comparison of the experimental spectra of amplitude fluctuations with the theoretical spectra, calculated for a model containing both strongly

anisotropic irregularities and isotropic Kolmogorov's turbulence, showed that a basic contribution is carried in the stratospheric amplitude fluctuations by the anisotropic irregularities, which correspond to the model of saturated internal gravity waves. The efficacy of the radio occultation technique for global remote monitoring of internal stratospheric waves has been shown. Analysis of phase and amplitude fluctuations in GPS/MET radio occultation data allows recovering information on the statistical properties of the atmospheric and ionospheric irregularities, which are connected with turbulence and wave processes. Information on the statistical irregularities is important to study processes of energy changes between the upper and lower atmosphere. Investigations in this direction are now in the early stage of development. The preliminary results are given describing the elaboration of the radio occultation method for the determination of turbulence and wave structures in the atmosphere.

4. A generalization of the radio holographic method for 3-dimensional implementation and inhomogeneous media is presented. The application of this method to radio occultation experiments allows obtaining 3-D images of the ionosphere, atmosphere and terrestrial surface. This leads to a more precise derivation of refractivity, temperature and vertical electron density gradients as well as a characterization of horizontal inhomogeneities of the atmosphere and ionosphere.

## Introduction

This report contains description of the results obtained in IRE RAS during the sixth stage of works owing to calendar plan of joint investigations with Potsdam Geophysical Scientific Center (GFZ-Potsdam). The plan of work that must be fulfilled in IRE RAS during the sixth stage consists in description main results of radio holographic method for delivering recommendation for its application for analysis radio occultation data. In the first section of this report the main features of radio holographic method is considered. Generalization of radio holographic method for three-dimensional (3-D) case is proposed. This generalization may be applied in future for developing polarization radio holography with aim of monitoring polarization-sensitive natural objects (rains, snow clouds etc.) in the Earth's atmosphere using signals, emitted by navigational and telecommunication satellites. It is shown that radio holographic method is a generalized form of backward propagation method. Radio holographic method in the proposed form may obtain, simultaneously, high vertical resolution and accuracy in estimation of the refraction angle and impact parameter. The effectiveness of radio holographic method was shown by means of revealing reflected signals in the GPS/MET and CHAMP radio occultation data. Combined radio holographic analysis of the phase and amplitude data allows observations of wave structures in the upper atmosphere and accurate measurements of the altitude profiles of the electron density and its vertical gradients in the D- and E- layers of the ionosphere. In the second part the results of measurements of turbulence parameters in the atmosphere is considered. Nowadays radio occultation method is applied basically for analysis of regular structures including information on altitudes profiles of the density, temperature, pressure and humidity in the atmosphere and electron density in the ionosphere. However radio occultation method allows recovering information on the statistical properties of the atmospheric and ionospheric irregularities, which are connected with turbulence and wave processes. Information on the statistical irregularities is important for study processes of energy changes between the upper and lower atmosphere. Investigations in this direction are now in the early stage of development. In the second part of the report the preliminary results are given describing elaboration of radio occultation method for determination of turbulence and wave structures in the atmosphere. In the conclusion the main results and recommendation for practical using of derived algorithms are given. The work planned for the GFZ/IRE-2001 contract is fulfilled in full volume.





## 1. Radio holographic method: Main results

### 1.1 Generalization of radio holographic method for three dimensional case

The geometry of radio occultation scheme is shown in Fig. 1.1. Navigational satellite GPS emitted radio waves, which propagated along two paths – (1 and 2 in Fig. 1.1). Reflected radio waves were registered with direct radio signal penetrated through atmosphere to receiver disposed on Low Orbital (LEO) satellite. The transmitter (GPS) and receiver were disposed correspondingly at point G and P with the distances  $R_2$ ,  $R_1$  from the center of spherical symmetry (point O). The angle between directions OG and OP is equal to  $\theta$ . The transmitter and receiver have different velocities  $v_G$  and  $v_P$ . The point D is the specular reflection point disposed on the smooth sphere of radius  $a$  corresponding to average Earth surface (Fig. 1.1). The direct and reflected signals are propagating through different parts of the ionosphere and atmosphere GP and GDP (Fig. 1.1). The receiver installed on LEO satellite registered phase and amplitude of radio waves at two frequencies F1, F2 corresponding to wavelengths 19 and 24 cm. Thus two radio holograms were obtained during every event of radio occultation experiment. The basic principles of the radio holography application to analysis of GPS/MET radio occultation data for recovering parameters of the atmosphere and ionosphere were described by *Pavelyev* [1998], *Hocke et al.* [1999], *Igarashi et al.* [2000]. For practical use it is necessary to obtain more general connections, which allow accounting for polarization properties of radio fields and, in principle, obtaining 3-D image of the ionosphere and atmosphere. Polarization effects may be observed in radio occultation data and, in principle, may be used for recovering clouds with rains, snow and other types of hydrometeors. Generalization of radio holography approach consists in application of vector equation given by Stratton and Chu [*Stratton, 1941*], for back-propagated field [*Pavelyev, 2001*]. Vector equation for radio holographic method has been obtained in the form:

$$\mathbf{E}(x', y', z') = - (4\pi)^{-1} \int_S [i\omega\mu(\mathbf{n}\times\mathbf{H})\phi + (\mathbf{n}\times\mathbf{E})\times\nabla\phi + (\mathbf{n}\cdot\mathbf{E})\nabla\phi] da. \quad (1.1)$$

$$\mathbf{H}(x', y', z') = (4\pi)^{-1} \int_S [i\omega\varepsilon(\mathbf{n}\times\mathbf{E})\phi - (\mathbf{n}\times\mathbf{H})\times\nabla\phi - (\mathbf{n}\mathbf{H})\nabla\phi] da. \quad (1.2)$$

where  $\mathbf{E}(x', y', z')$  and  $\mathbf{H}(x', y', z')$  are the backward propagating electromagnetic fields at an interior point  $(x', y', z')$  of inhomogeneous medium in terms of the known fields  $\mathbf{E}$  and  $\mathbf{H}$  over a surface  $S$ , and  $\phi$  is the Green function, corresponding to backward propagating field. The Green function  $\phi$  may be found from wave equation, corresponding to inhomogeneous medium:

$$\Delta\phi + k^2\phi = \delta(\mathbf{r}-\mathbf{r}') \quad (1.3)$$

where  $\delta(\mathbf{r}-\mathbf{r}')$  is delta-function. For homogeneous media the backward solution of (1.3) has a form:

$$\phi = e^{-ikr}/r \quad (1.4)$$

for time dependence of the field assumed in the form  $\exp(-i\omega t)$ , where  $\omega$  is circular frequency of monochromatic signal. Equations (1.1), (1.2) are written in MKS units system. For Gauss units system these equation may be written in the form:

$$\mathbf{E}(\mathbf{P}_i) = ik(4\pi)^{-1} \iint dS \mathbf{Q}_E(\mathbf{E}, \mathbf{H}); \mathbf{Q}_E(\mathbf{E}, \mathbf{H}) = \{(\mathbf{n} \times \mathbf{H})\phi + [(\mathbf{n} \times \mathbf{E}) \times \nabla \phi + (\mathbf{n} \cdot \mathbf{E}) \nabla \phi] / (ik)\}, \quad (1.5)$$

$$\mathbf{H}(\mathbf{P}_i) = ik(4\pi)^{-1} \iint dS \mathbf{Q}_H(\mathbf{E}, \mathbf{H}); \mathbf{Q}_H(\mathbf{E}, \mathbf{H}) = \{(\mathbf{n} \times \mathbf{E})\phi - [(\mathbf{n} \times \mathbf{H}) \times \nabla \phi - (\mathbf{n} \cdot \mathbf{H}) \nabla \phi] / (ik)\}. \quad (1.6)$$

Equations (1.5), (1.6) give a general presentation for backward propagating fields, if the fields at some surface  $S$  are known and the point of observation is located inside inhomogeneous medium. For determining of the backward propagating field it is necessary to find the Green function  $\phi$  by means of solving wave equation (1.3). For solution of (1.3) asymptotic method may be applied and  $\phi$  may be found in the form:

$$\phi = A e^{-i\Phi}; \quad \Phi = k_0 \int n dl \quad (1.7)$$

where  $\Phi$  and  $A$  are the phase and amplitude of Green function,  $k_0$  is the free space wave number,  $n$  is the refraction index of the medium, and integration in (1.7) is provided along the ray connecting observation point  $(x', y', z')$  and element  $da$  on the surface  $S$ . For the case of isotropic media  $\Phi = kr$ ,  $A = 1/r$  and one may obtain from (1.5), (1.6):

$$\mathbf{E}(\mathbf{P}_i) = ik(4\pi)^{-1} \iint dS R_d^{-1} \exp(-ikR_d) \mathbf{Q}_E(\mathbf{E}, \mathbf{H}); \quad \mathbf{Q}_E(\mathbf{E}, \mathbf{H}) = [\mathbf{nH}] - [[\mathbf{nE}]\mathbf{g}_-] - (\mathbf{nE})\mathbf{g}_-, \quad (1.8)$$

$$\mathbf{H}(\mathbf{P}_i) = ik(4\pi)^{-1} \iint dS R_d^{-1} \exp(-ikR_d) \mathbf{Q}_H(\mathbf{E}, \mathbf{H}); \quad \mathbf{Q}_H(\mathbf{E}, \mathbf{H}) = [\mathbf{En}] - [[\mathbf{nH}]\mathbf{g}_-] - (\mathbf{nH})\mathbf{g}_-, \quad (1.9)$$

$$\mathbf{g}_- = (1 - i/kR_d) \mathbf{grad} R_d, \quad R_d = [(x - x')^2 + (y - y')^2 + (z - z')^2]^{1/2} \quad (1.10)$$

where  $(x, y, z)$  are coordinates of element  $da$ .

Formulas (1.5), (1.6) are the basic radio holography equations for three-dimensional case and inhomogeneous medium. Equations (1.8)-(1.10) restore electromagnetic field inside homogeneous part of the volume  $V$  if the fields  $\mathbf{E}$ ,  $\mathbf{H}$  are known at the interface  $S$ . It may be noted that information on the field distribution at some part of the surface  $S$  may be used for constructing image of refractive volume as follows from holography practice known in optics. Spatial resolution depends on the size of the part of the interface  $S$  where the field distribution is given. One may obtain an equation corresponding to two-dimensional case using equations (1.8)-(1.10). This equation describes the field in some plane inside the volume  $V$  as function of the field along a given curve  $L$  in the same plane as shown by *Pavelyev* [2001]:

$$\mathbf{E}(\mathbf{P}_i) = (k/2\pi)^{1/2} \int dL R_d^{-1/2} \cos \theta \exp(i\pi/4 - ikR_d) \mathbf{E}_o \quad (1.11)$$

where  $\theta$  is the angle between normal to the curve  $L$  and direction to the point of observation. Equation (1.11) is a basic for practical implementation of the radio holographic method when experimental data  $\mathbf{E}_o$  are given along the LEO orbit as function of time. In this case polarization effects may be applied for monitoring the objects in the ionosphere and atmosphere, which change polarization state of radio waves.

## 1.2 Radio holographic method as generalized form of backward propagation method

Usually the back-propagated field  $u(x,y,z)$  is calculated using the diffractive integral [Vladimirov, 1971; Gorbunov et al., 1996]:

$$u(x,y,z)=(k/2\pi)^{1/2}\int dS_y |\mathbf{r}-\mathbf{y}|^{-1/2} \cos\varphi_{ry} \exp(i\pi/4-ik|\mathbf{r}-\mathbf{y}|)u_o(\mathbf{y}); \quad (1.12)$$

where  $\mathbf{r}$ ,  $\mathbf{y}$  correspond to coordinates of the observation point  $P_i$  and the current point of integration on the curve  $L$  coinciding with LEO orbit;  $\varphi_{ry}$  is the angle between vector  $\mathbf{r}-\mathbf{y}$  and normal  $n_y$  to curve  $L$  at current integration point  $\mathbf{y}$ , and  $u_o(\mathbf{y})$  is scalar field measured along the orbit of LEO satellite. Equation (1.12) has been derived under assumption that the source of the wave field (GPS) is stationary and that the LEO orbit is located in vertical plane, which may be referred to as the occultation plane [Gorbunov, 2001]. Comparison of equations (1.11), (1.12) shows their coincidence for homogeneous media. For inhomogeneous media equation (1.11) must be changed to asymptotic formula:

$$\mathbf{E}(P_i)=(k/2\pi)^{1/2}\int dL A \cos\theta \exp(i\pi/4-i\Phi)\mathbf{E}_o; \quad \Phi=k_o\int ndl; \quad A=X/r^{1/2} \quad (1.13)$$

where  $X$  is the refraction attenuation on the ray path between the observation point and current integration point. Equation (1.13) generalizes the main backward formula (1.12) for inhomogeneous case. Both formulas (1.12), (1.13) may be applied to determination of the field between LEO satellite and ionosphere, where the refraction index is constant,  $n=1$ . Formally one may use (1.12) for back-propagation in the inhomogeneous media, however the recovered fields may be different from real fields distribution inside the atmosphere. Thus back-propagation method in the form suggested by Gorbunov et al., [1996], is limited in application by homogeneous region between the LEO orbit and atmosphere. The radio holographic approach may be used for restoration radio fields inside the atmosphere. This possibility is connected with appropriate construction of reference signal. Equation (1.13) contains the measured radio field  $\mathbf{E}_o$  and complex function  $S(x,y,z)$ :

$$S(x,y,z)=A \cos\theta \exp(i\pi/4-i\Phi). \quad (1.14)$$

The function  $S(x,y,z)$  may be considered as a reference signal, which is used for restoration radio field in any point of volume disposed between the LEO orbit and GPS transmitter. The phase of reference signal  $\Phi=kr$  for homogeneous part and  $\Phi=k_o\int ndl$  for inhomogeneous part of the volume. Thus for restoration of the radio field inside the atmosphere some information on the refraction index distribution must be used. In general case the radio field along the LEO orbit may be considered as a sum of signals with different origin:

$$\mathbf{E}_o = \sum_m \mathbf{E}_{om} \exp(i\Phi_m), \quad (1.15)$$

where the summation index  $m$ , amplitudes  $\mathbf{E}_{om}$  and phases  $\Phi_m$  correspond to signals of different kinds (refracted, diffracted, reflected, scattered etc.). Inserting (1.15), (1.14) to (1.13) gives:

$$\mathbf{E}(P_i)=(k/2\pi)^{1/2}\int dL \sum_m \mathbf{E}_{om} \exp(i\Phi_m) S(x,y,z). \quad (1.16)$$

The main task of radio occultation is to find the amplitude and phase of each member in the sum (1.15) and then to find the physical properties of media, which correspond to this term.

Usually only refraction term is revealed from radio occultation data. Then vertical profiles of the refractive index, temperature, pressure, geo-potential, and humidity may be determined. Recovering signals reflected from the Earth surface is important for bistatic scatterometry of the Earth surface and for study of boundary layer of the atmosphere. Observation of multibeam propagation, caustic boundaries, wave-guide propagation, gives experimental data for fundamental theory of radio waves propagation. Recognition of signals scattered from turbulence layers are important for practical meteorology and for revealing zone of breaking internal waves and heat exchange inside the atmosphere. Polarization analysis of different terms in (1.16) may be interesting for recovering ionospheric effects, clouds and hydrometeors phenomena in the atmosphere. The main idea of radio holographic method consists in revealing each term in the sum (1.16) by means of appropriate choose of function  $S(x,y,z)$ . The function  $S(x,y,z)$  must be coherent with corresponding term in (1.16). For recovering refracted term in (1.16) the function  $S(x,y,z)$  according to *Pavelyev et al.*, [1996], *Hocke et al.* [1999], *Igarashi et al.* [2000], has been chosen in the form:

$$S(x,y,z)=\exp(-i\Phi), \quad \Phi=k_0\int ndl \quad (1.17)$$

where integration is fulfilled along the ray path between the current point on the LEO orbit and GPS transmitter. The refraction index  $n(l)$  corresponds to radio physical model of the atmosphere described by *Pavelyev et al.* [1996]. Parameters of the radio physical model are usually chosen to be corresponding to expected meteorological conditions in a radio occultation region. If the chosen model is accurate then the effect of maximum spatial compression of radio occultation signal is achieved. In this case the modeled field distribution coincides with experimental field measured along the LEO orbit. According to (1.16), (1.17) and (1.11) the physical sense both of the backward method and radio holographic approach consists in optimal open-loop phase tracking of the radio occultation signal. The backward method uses open-loop phase tracking with phase  $\Phi=kr$ , where  $r$  is the distance between a current point on the LEO orbit and an observation point in the free space. The aim of backward method is to find the field distribution in the single-ray area between LEO orbit and the atmosphere and then use single-ray approximation for determination of the impact parameter and refraction angle. The radio holographic method uses open-loop phase tracking with phase  $\Phi=k_0\int ndl$  where dependence  $n(r)$  is known from model describing expected altitude profile of the refraction index in the atmosphere. The phase integral corresponds to the phase path between a current point on the LEO orbit and an observation point disposed in any area between the receiver and transmitter (including the atmosphere). Thus radio holographic approach may be considered as a generalized form of the backward method. So the radio holographic method may be used for recovering field distribution inside the atmosphere and ionosphere. However it is more effective to use radio holographic approach for direct measurement of main parameters of refracted component of radio occultation signal: the impact parameter and refraction angle. For this aim the phase path is chosen to be connecting directly a receiver and transmitter in radio holographic approach. This form of phase tracking is better for revealing the refracted (or reflected) signals, which are in coherence with reference signal. This allows high-precision estimation of the impact parameters and refraction angle of the refracted and reflected signals. The radio holographic approach does not contain limitations between precision in determination of the impact parameter and refraction angle.

### 1.3 Validation of radio holographic method by means of observation of reflected signal in GPS/MET radio occultation data

Radio holographic method may be applied also for recovering radio signals reflected from the Earth surface as was shown by *Beyerle and Hocke* [2001], *Pavelyev et al.* [2001], *Igarashi et al.* [2001]. The reflected signal in GPS/MET radio occultation data has been discovered by radio holographic method five years ago after beginning radio occultation experiment GPS/MET. The first application of radio holographic method to analysis of GPS/MET radio occultation data give direct evidences of multibeam propagation and recovered in some radio occultation events signals, reflected from the Earth surface. Reflected signal may be used in future as additional information source for radio occultation data analysis. The radio holographic approach allows simultaneous high-precision measurements of the impact parameter and refraction angle corresponding to main refracted ray. The achieved angular and height precision may be illustrated in Fig. 1.2. As an example of high vertical resolution of radio holographic method, the results of an application of the radio holographic approach to the analysis of GPS/MET radio occultation data (event No.0392, February 05, 1997) are shown in Fig. 1.2. The vertical distribution of radio brightness in the mesosphere (left upper panel in Fig. 1.2) reveals sharp peak corresponding to the main ray. The width of this peak on the half power level gives magnitude of vertical resolution of radio holographic method  $\sim 70$  m. This value corresponds to angular resolution of about 0.035 mrad at a horizontal distance 2000 km. The radio brightness distribution in the troposphere at a level of 2 km is shown in Fig. 1.2 (upper right panel and the two lower panels). The two prominent features, representing the multibeam propagation in the troposphere and the signal, reflected from the sea's surface, have spikes with width of about 70 m. Small spikes disposed on the main peaks in Fig. 1.2 (upper right and two panels below) show even more sharp widths about of 30-50 m. The weak reflected signal with level of about 20 dB below the combined power of the main peaks is revealed clearly despite it is not seen directly in the phase and amplitude of radio occultation signal. So radio holographic method demonstrated important property to reveal weak signal disposed at small vertical distance relative the main ray on the phone of much powerful signal (which may be considered as an interference) and shown high filtration ability greater than 20 dB. Results shown in Fig. 1.2 demonstrated the effectiveness of application of radio holography method for measurements of angular spectra and spatial filtration of radio occultation signal.

## 1.4 Comparing vertical resolution of the radio holographic and backward methods

The basic principles of the radio holography application to analysis of GPS/MET radio occultation data for recovering parameters of the atmosphere and ionosphere were described by *Pavelyev [1998]*, *Hocke et al. [1999]*, *Igarashi et al. [2000]*. Their approach consists in application focused synthetic aperture method to analysis of radio hologram measured along orbital trajectory of receiving satellite. This method gives a possibility for accurate simultaneous evaluation of the refraction angle and impact parameter corresponding to each ray in the angular spectrum of radio waves along satellite orbit. Because layered structure of the ionosphere and atmosphere this approach gives high vertical resolution and accuracy in estimation vertical profiles of physical parameters. Thus focused synthetic aperture method reveals 2-D image of the ionosphere and atmosphere as seen from the low orbital satellite. As shown by *Igarashi et al. [2000]* the angular resolution of radio holographic approach  $\Delta\beta$  depends on the time  $T$  of coherence of reference signal and signals refracted in the ionosphere and atmosphere. If  $T$  increases, the angular resolution in the angular spectrum increases and  $\Delta\beta$  diminishes. Resulting resolution in the angular spectrum  $\Delta\beta$  and corresponding vertical resolution  $\Delta h$  can be found from:

$$\begin{aligned} \Delta\beta &= \lambda \Delta f / \{2v\}, \quad \Delta f = 1/T, \quad \Delta\beta = \pi / (Tk v), \quad \Delta h = \Delta p = L \Delta\beta, \\ L &\approx (r^2 - p^2)^{1/2}, \quad \Delta\xi \Delta p \approx L [\pi / (Tk v)]^2, \quad v = r d\theta / dt \end{aligned} \quad (1.18)$$

where  $k = 2\pi/\lambda$ ,  $\theta$  is the angle between the low-orbital (LEO) and navigational satellite as seen from the center of spherical symmetry of the atmosphere,  $r$  is distance the LEO and the center of spherical symmetry. According to equation (1.18) the accuracy of the radio holographic method increases when  $v$  and  $T$  are growing and the wavelength is diminishing. The wavelength dependence of angular resolution, equation (1.18), is distinct from the Fresnel one:  $\Delta\beta$  (radio holographic)  $\sim \lambda$  and  $\Delta\beta$  (Fresnel)  $\sim \lambda^{1/2}$ . Due to this difference, the radio holographic method seems to be an effective tool for radio occultation data analysis. According to (1.18) it may be possible to have simultaneously high resolution on the impact parameter and refraction angle  $\Delta\xi$ ,  $\Delta p$ . This resolution may be compared with resolution corresponding to quantum cell approach developed by *Gorbunov et al. [2000]*

$$\Delta\xi = \lambda/A, \quad \Delta p = A/\zeta, \quad \Delta p \Delta\xi \sim \lambda/\zeta \quad (1.19)$$

where  $A$  is the optimal aperture size corresponding to spatial spectral resolution  $\Delta k = 2\pi/A$ ,  $\zeta$  is the refraction attenuation,  $\zeta$  is of order of unity for the weak refraction case. According to quantum cell approach the uncertainties of refraction angle and impact parameter are estimated as  $2.6 \cdot 10^{-4}$  rad and 800 m respectively for the observation distance  $\sim 3000$  km and the wavelength  $\sim 20$  cm [*Gorbunov et al., 2000*]. The resolution corresponding to radio holographic method may be described by approximate equations:

$$\begin{aligned} \Delta\xi &\approx \Delta\beta = \lambda/2l_s; & \Delta p &= L\lambda/2l_s; & \Delta\xi \Delta p &\approx L\lambda^2/(4l_s^2), \\ l_s &= Tv \text{ (radio holographic approach)} \end{aligned} \quad (1.20)$$

where  $l_s$  is the focused synthetic aperture length. For radio holographic approach the corresponding uncertainties are: 4...8 micro radians and 10-20 meters respectively. It follows from comparison (1.19), (1.20) that radio holographic method gives better resolution than quantum cell approach. It follows from this analysis that the angular resolution of the radio

holographic method may achieve 3-5 micro radians. It may be noted that there exists a deep analogy between the focused synthetic aperture method applied to high resolution radar imaging (see, for example, *Wehner* [1987], section 6.4 SAR Theory (Focused Aperture)) and the radio holographic approach, except the only difference: a target in the radio occultation case are refracted rays, moving through the atmosphere. The main requirement in both cases is coherence time interval of reference signal  $T$  with signals from targets. Time  $T$  of coherence with refracted signals depends on coincidence of radio physical model used for construction of reference signal to physical state of the atmosphere. For achieving maximum in spatial resolution adaptive procedure may be used which changes parameters of radio physical model to account for refraction and diffraction effects in the atmosphere. Adaptive procedure requires accurate solution of direct and inverse problem of radio occultation. This may be considered as maximum spatial compression of the radio occultation signal. For fulfilling this requirement the refractivity altitude dependence used in the radio physical model must be close to the real height dependence of the refractive index in the radio occultation region. If the used model of a target is accurate then extreme instrumental spatial resolution may be achieved (one half of the real antenna's aperture in the radar case as it described by *Wehner*, [1987], the angular accuracy  $\Delta\beta$  and vertical resolution  $\Delta h$  from (1.20) in the radio occultation case). Adaptive procedure must work in real time for assimilating radio holographic data with subsequent use in meteorology and space weather application. This requires constructing new radio holographic algorithms, which use effective processes of solution of direct and inverse refraction and diffraction problem for inhomogeneous media. Also appropriate algorithms must be developed, which account for horizontal gradients.

Focused synthetic aperture method gives full solution of the task of the backward propagation approach (derived by *Gorbunov et al.* [1996], *Karael and Hinson* [1997], *Mortensen et al.* [1999]) because determination of the phase and amplitude of each ray in the angular spectrum allows recovering radio fields between the orbit of LEO satellite and atmosphere. However focused synthetic aperture method gives directly vertical profiles of physical parameters in the ionosphere and atmosphere without intermediate stage of recalculating radio fields from LEO orbit to phase screen near the atmosphere. Excluding intermediate stage allows constructing practical algorithms for solution inverse radio holographic problem, which work in real time. Developing new practical procedures of radio holographic analysis of radio occultation data is a task for future investigation.

## 1.5 Observation of wave structures in the upper atmosphere by radio holographic method

As examples of effectiveness of radio holographic method the results of the first observation of wave structures in the upper atmosphere may be considered. To obtain the wave part of the radio hologram it is necessary to reveal regular part in the phase corresponding to reference beam for subsequent subtraction from experimental data as described by *Igarashi et al.* [2000]. This may be done using IRI-95 model describing expected electron density profile for the time and place of radio occultation experiment. The results of calculations of the phase of reference beam for frequencies F1 and F2 are given in Fig. 1.3 (left panel) for GPS/MET event 0393 (February 14, 1997; 13 h 56 m 23 s UT; 29.5° N, 223.9° W). The excess phase path corresponding to reference beam at two frequencies F1, F2 is described by the curves 1 and 3 in Fig. 1.3. Experimental data are shown by the curves 2 and 4 in Fig. 1.3. The results of calculations show good correspondence between calculated and experimental data. Deflections from the calculated curves are not higher than  $\pm 1$  cm in the height interval 65-112 km. The feature in the height interval 55-65 km may be connected with influence of horizontal gradients in the ionosphere because the amplitude of deflections from regular contribution depends on frequency according to usual ionospheric square law. The horizontal gradients arisen at the ray path LEO satellite and the ray turning point in the atmosphere (night part of the ionosphere) and at the ray path turning point in the atmosphere – GPS satellite (evening part of the ionosphere). The horizontal gradients appeared because in the night ionosphere regular electron density is lower than in the evening ionosphere. The results of restoration of the vertical distribution of the electron density for event 0393 are shown in Fig. 1.3 (right panel). The two maximums in the electron density is of about  $15 \cdot 10^9$  [1/m<sup>3</sup>]. Also the secondary maximums are seen in the Fig. 1.3 (right panel). The results shown in Fig. 1.3 illustrate accuracy of radio holographic approach for solution inverse problem. The origin of this accuracy consists in independent construction of reference beam with subsequent using perturbation method for retrieval of deflections in the experimental profile relative a model profile.

The amplitude and phase components of radio holograms of the D-region of the ionosphere that correspond to four GPS/MET occultation events (February 14, 1997, No. 0046-left upper panel; February 07, 1997, No. 0447, 0158 - right upper and left lower panels; October 25, 1995 No. 0033 - right lower panel) are shown in Fig. 1.4. Occultation events No. 0046, 0447 took place near Japan (Okinawa) in the middle daytime and in the middle of nighttime respectively. The time-spatial coordinate of the main ray's minimal height  $H$  were close to 28.5°N, 210.5°W, 01 h 43 m 33 s UT and 25.5°N, 231.7°W, 15 h 53 m 23 s UT correspondingly. The third event (07 February 1997, No. 0158) corresponds to summer daytime in the Antarctic region. The time-spatial coordinates of ray minimal height  $H$  varied from 71.2°S, 18.2°W,  $H=95$  km, 14 h 51 m 05 s UT to 70.5°S, 16.4°W,  $H=60$  km, 14 h 51 m 25 s UT. The fourth event take place above Andes Mountains region (South America) at 34.0° S, 71.7° W, 01 h 10 m 43 s UT at the local evening time.

The two curves in the middle of panels of Fig. 1.4 correspond to the experimental excess phase variations at the first frequency F1,  $S_1$  (upper curve), and at the second frequency F2,  $S_2$ , as functions of height. These curves have been multiplied and displaced to make more visible the variations, that are connected with the wave structures. The upper ionospheric contribution was subtracted from the excess phase data by using the IRI-95 F-layer model for time and region of radio occultation. The variations in amplitude (top and bottom pairs of



curves in Fig. 1.4) are strongly correlated. The level of variations in the phase-path excess and in amplitudes at the two frequencies is proportional to the ratio  $f_2^2/f_1^2$ , and this demonstrates that the variations originate due to fluctuations in the electron density.

The phase excess changes in the interval  $\pm 1$  cm, with a random noise contribution of about  $\pm 1$  mm. Spatial periods in the 1-3 km range can clearly be seen in the excess phase data of Fig. 1.4. A spatial period of 5 km can more clearly be seen in the excess phase data for Antarctic event than in the data for Okinawa events. In the amplitude data (top and bottom pairs of curves in Fig. 1.4) spatial periods in the 0.5-2 km range can also be seen. A feature at the height of 72 km (And event) and 78 km (Antarctic event) is seen in both the phase excess and amplitude data.

Analysis of Fig. 1.4 indicates that the amplitude data are more sensitive to high spatial frequency components in the refractive index while the phase excess data are more sensitive to low frequency components. These variations could correspond to wave structures in the electron density distribution in the D-layer of the ionosphere. The vertical gradient of electron density may be retrieved from the amplitude data by a method, which has been described by *Igarashi et al.* [2000]. The results of the restoration  $dN_e(H)/dH$  for four events 0033, 0046, 0447 and 0158 are shown in Fig. 1.5. For the ease of comparison, the curves have been displaced by  $20 \cdot 10^9$  [ $1/m^3 km^{-1}$ ]. The spatial periods for Ocinawan event are somewhat shorter by a factor of about two than the periods for another events. The amplitude of the waves over Okinawa is also greater, indicating a more intense process. The maximum value of the positive gradient is at a height of about 76 km. It follows from Fig. 1.5 that the wave structures in the D-layer seem to be quasi-sinusoidal with slow changes in the amplitude and frequency. This indicates on possible existence of only two-three propagated modes as was suggested by *Sica and Russel* [1999] from analysis lidar data. For example, for the event 0033, the changes in the vertical period of the wave by two times from 2 km to 1 km may be seen by comparing the vertical gradient of the electron density variations in the height intervals 65-70 km and 74-79 km. High amplitude values  $\sim 8-10 \cdot 10^9$  [ $1/m^3 km^{-1}$ ] near 72 km (0033 event), 75-80 km (0046 event), 77-80 km (0158 event) and 66, 70-72, 77, 80 km (0447 event) may be connected with physical conditions of internal waves propagation. The strong features, which are seen in the height ranges 70-80 km (Okinawan event) and 75-80 km (Antarctic event), may correspond to breaking of internal waves in a region near the temperature inversion that is usually observed at this altitude by Earth-based radar and lidar tools [*Hauchecorne et al.*, 1987]. Another example may be seen in Fig. 1.6, 1.7 for GPS/MET occultation event No. 79. The event 09 February 1997, No. 79, corresponds to winter daytime at the north part of Pacific Ocean near Japan. The time-spatial coordinates of ray minimal height  $H$  varied from 48.1°N, 226.8°W,  $H=112$  km, 07 h 19 m 53 s UT to 47.5°N 2267.4°W,  $H=60$  km, 07 h 20 m 25 s UT. The two curves below in the Fig. 1.6 correspond to the experimental phase excess variations at the first frequency F1, (upper curve), and at the second frequency F2, as functions of height. Both curves are multiplied by factor 2. The variations in amplitude (top pair of curves in Fig. 1.6) are also strongly correlated. The level of variations in the phase-path excess and in amplitudes at the two frequencies is proportional to the ratio  $f_2^2/f_1^2$ , and this demonstrates that the variations originate due to fluctuations in the electron density. The phase excess that are connected with wave structures change in the interval  $\pm 2$  cm, with a random noise contribution of about  $\pm 1$  mm. Spatial periods in the 1...3 km range can be seen in the phase excess data of Fig. 1.6. The spatial periods in the 1...2 km range can be clearly observed in the amplitude data. A feature at the height interval 72...78 km is seen in both the phase excess and amplitude data. These variations correspond to wave structures in the electrons density distribution in the D-layer of the ionosphere. The results of the restoration  $dN_e(H)/dH$  for event 79 are shown in Fig. 1.7, left curve. This profile reveals wave-like structures in the D-layer plasma with a spatial period of 1-2 km and variations in the electron density gradient

from  $\pm 3 \cdot 10^3$  to  $\pm 6 \cdot 10^3$  electrons/(cm<sup>3</sup>km). The main peak in the D-layer gradient is observed at  $H=75$  km with a value of  $8 \cdot 10^3$  electrons/(cm<sup>3</sup>km). This peak is also clearly seen in the amplitude part of radio hologram (Fig. 1.6). Sharp spike in the vertical distribution of the electron density at the height 106 km corresponding to sporadic E-layer is seen in Fig. 1.7, right curve (displaced for comparing at  $30 \cdot 10^3$  electrons/(cm<sup>3</sup>km)). The electron density altitude profile may be obtained by using dependence of  $dN_e/dH$  on height under certain initial condition, for example,  $N_e(H)=0$  if  $H=69$  km. The resulting electron density vertical distribution is shown in Fig. 1.7, right curve. The main cause of the waves observed in the vertical profiles of electron density may be internal waves. The perturbations observed in the vertical profiles of electron density might have a different origin. They may be connected with temperature waves caused by internal waves which amplitude grows with height.

The power spatial spectra of the vertical gradient of refractivity (N-units/km) that correspond to the variations in the gradients of electron density are shown in Fig. 1.8. The curves (displaced for ease of comparison by 40 db) show the separate power spatial spectra  $W(2\pi/\Lambda)$  (expressed in [N-units]<sup>2</sup>), multiplied by  $10^6$ , for all four events as function of spatial frequency  $2\pi/\Lambda$  (expressed in km<sup>-1</sup>). A comparison of the four events reveals flat region in the spatial spectrum with spatial periods between of about 1.6 and 10 km. The straight lines in Fig. 1.6 show the slope of the spectra in the high frequency region. The slope of the spectra in the high spatial frequency region and other parameters of the spectra are given in the Table 1.

Number of event	Power degree, n
0447	-3.0±0.3
0158	-2.2±0.3
0046	-2.3±0.3
0033	-3.1±0.3

**Table 1.** Parameters of the spectra of the refractivity gradient in the D-layer.

The power degree in the high frequency part of the spectrum is practically the same for all events (near  $n_s=-3$ ). The power degree for all events is very near to the slope in the tail spectrum of internal waves as described by Tsuda et al. 1991. So the variations in the electron density vertical profile may be connected with influence of internal waves propagated in the neutral atmosphere.

## 2. Development of method for monitoring of statistical atmospheric and ionospheric irregularities using radio occultation method

### 2.1 Phase fluctuations at $\lambda=19$ cm (GPS/MET experiment)

Stochastic changes of phase and amplitude, caused due to fluctuations of the refractive index are registered in radio occultation experiments. The ionospheric and atmospheric phase fluctuations limit accuracy of the estimation of the atmospheric parameters (temperature, humidity etc.). Analysis of the amplitude and phase fluctuations is important because the appropriate experimental data can give the information about turbulent and wave phenomena in atmosphere and ionosphere.

Analysis of the amplitude and phase fluctuations was given by *Yakovlev et al.*, [2000] for MIR/GEO radio occultation experiments at wavelength 2 cm. Their work demonstrated a possibility of measurements of parameters of statistical irregularities in the atmosphere by radio occultation method. High- stability of radio occultation signal allows to carry out investigations of the amplitude and phase fluctuations of radio waves in decimeter band. *Yakovlev et al.*, [2000] provided preliminary analysis of the amplitude and phase fluctuations using GPS/MET radio occultation data. For developing of radio occultation method of monitoring of small-scale irregularity of the atmosphere the results of joint analysis of the amplitude and phase variations are necessary.

Aim of this section consists in analysis of the amplitude and phase fluctuations of radio waves propagated through the atmosphere registered in the GPS/MET radio occultation experiments.

The primary experimental data contain results of phase measurement at  $\lambda_l=19$  cm with sampling rate equal to 50 Hz on temporal intervals about of 40 s. The minimum height of a ray path,  $CD=H_0$ , changes from 60 up to 2 km. Ray path geometry is shown in Fig. 2.1. The rate of change of minimal height,  $V_B = dH_0/dt$  in ionosphere and stratosphere was equal to  $1.7\div 2.5$  km  $s^{-1}$ . In the troposphere in different radio occultation events of measurement it was equal to  $0.45\div 0.7$  km  $s^{-1}$  because refraction. Phase changes have large regular  $\varphi_0(H_0)$  and small stochastic  $\delta\varphi(H_0)$  components. Component  $\varphi_0(H_0)$  is caused by altitude dependence of the refractive index  $N(h)$  in radio occultation region, and stochastic component is connected with statistical fluctuations  $\delta N(h, t)$ , caused by turbulence, and irregular layered structures. It is known [*Ishimaru*, 1978], that large-scale components of a spatial spectrum of the refractive index introduces basic contribution in phase fluctuations. According to *Yakovlev et al.*, [1996], *Dalaudier et al.*, [1994], external scale  $L_0$  of atmospheric irregularities, causing phase fluctuations, is equal to 3 km. Therefore the minimum duration  $\Delta T$  of realization of phase measurements, necessary for correct determination of the phase dispersion  $\sigma_\varphi^2$ , should be about  $2L_0/V_B$ , where  $V_B$  is the vertical velocity with which a radio occultation ray crossed atmospheric irregularities. In our case  $\Delta T \approx 4$  s, this is only ten times lower than duration of radio occultation experiment. The height interval of  $\Delta H_0$ , corresponding to  $\Delta T=4$  s, was equal  $7\div 10$  km in the stratosphere and about  $1.8\div 2.6$  km in the troposphere. We were compelled to choose short temporal intervals  $\Delta T$ . This limited the magnitude of greatest scale which gives contribution in dispersion value  $\sigma_\varphi^2$ . Thus, at the analysis of atmospheric effects, determination of the characteristics of irregularities with greatest scale  $l = \Delta TV/2 \approx 4$  km was possible.

For determination of fluctuation component  $\delta\varphi$  we found by the least squares method the regular changes of phase  $\varphi_0(H_0)$  on interval  $\Delta H_0$  using polinom of the second degree. Then we subtracted  $\varphi_0(H_0)$  from experimental phase temporal dependence. The obtained stochastic function  $\delta\varphi(t)$  had zero average value. Then we found phase dispersion,  $\sigma_1^2$ , for interval  $\Delta H_0$ . 8-10 values of dispersion  $\sigma_1^2$  were obtained in result of primary data processing for each occultation. At the analysis the atmospheric phase fluctuations influence and technical instability of phase should be taken into account. For exception of the contribution of these independent stochastic components we determined phase dispersion  $\sigma_2^2$  for height interval  $H_0=40\div 50$  km, where influence of the neutral atmosphere can be neglected. We found dispersion of atmospheric phase fluctuations  $\sigma_\varphi^2$  using difference  $\sigma_\varphi^2 = \sigma_1^2 - \sigma_2^2$ . Data of 52 radio occultation events, carried out in February 1997 in regions bounded by coordinates  $23^0\div 60^0$  N and  $120^0\div 150^0$  E were processed for analysis of ionospheric and atmospheric irregularities.

The atmospheric phase fluctuations can be characterized by the root-mean-square (RMS) deviation  $\sigma_\varphi$ , expressed in radians, or appropriate fluctuations of the eikonal  $\sigma_\psi$ , having dimension of length. Eikonal  $\sigma_\psi$  and the phase  $\sigma_\varphi$  are connected by equation  $\varphi = (2\pi/\lambda)\psi$ , and appropriate RMS values are also connected by formula  $\sigma_\varphi = (2\pi/\lambda)\sigma_\psi$ . Values  $\sigma_\psi$  do not depend on wavelength;  $\sigma_\varphi=0.33$  rad corresponds to  $\sigma_\psi=1$  cm. The experimental dependences  $\sigma_\psi$  from height  $H_0$  are submitted in Fig. 2.2 and 2.3 accordingly for the stratosphere and troposphere. The stratospheric fluctuations begin to be registered from height  $H_0=36$  km; for  $H_0=30$  km  $\sigma_\psi$  was equal 2.3 mm on the average, at further reduction of  $H_0$  monotonous increase of  $\sigma_\psi$  occurs, so for  $H_0$ , equal to 20 and 14 km the average values  $\sigma_\psi$  are accordingly equal to 9 and 16 mm. In separate radio occultation strong increase of  $\sigma_\psi$  at heights 22...24 km was observed. In the troposphere  $\sigma_\psi$  increased on the average up to  $\sigma_\psi=44$  mm for  $H_0=3$  km. At the height  $H_0=6$  km regular increase  $\sigma_\psi$  is also observed for part of events. The experimental data submitted in Fig. 2.2 and 2.3 are obtained during time interval of one month, thus in different days strong difference  $\sigma_\psi$  for the same heights was registered. The maximum and minimum values  $\sigma_\psi$  are shown on these figures by a dotted line, and the average dependence  $\sigma_\psi(H_0)$  is given by continuous curve. In Fig. 2.2 and 2.3 the scattering of experimental values  $\sigma_\psi$  is caused by variability  $\sigma_\psi$ , instead of errors of measurements. We estimate errors of determination  $\sigma_\psi$  as magnitude about of 1 mm for the altitude interval 20...34 km and 4 mm for  $H_0=4...18$  km.

Below we shall analyze spectra of atmospheric fluctuations of eikonal  $G_\psi(F)$ , where  $F$  is the fluctuations frequency. We determined spectrum  $G_\psi(F)$  during time interval  $\Delta T=5$  s for the stratospheric and tropospheric heights intervals. For analysis of fluctuations in the stratosphere and troposphere the heights intervals 15...24 km and 4...7 km were used. The tropopause region, which usually introduces significant regular change of eikonal, was excluded from the analysis. The spectra  $G_\psi(F)$  were determined by method of fast Fourier transform (FFT) with subsequent smoothing within rectangular window of width  $\Delta F=F/2$ . In Fig. 2.5 examples of experimental spectra fluctuations of eikonal are shown. The group of spectra 1 corresponds to the troposphere, and group 2 it is to the stratosphere. The experimental spectra are well described by power dependence  $G_\psi(F) \propto F^m$ . It is found, that for the troposphere average value of index  $m$  is equal to  $m=2.2\pm 0.4$ , and for the stratosphere  $m=2.6\pm 0.5$ . As follows from theory of radio waves propagation in random media [Ishimaru, 1978], index  $m$  is connected with index  $p$  of spatial spectrum of fluctuations of the refractive index by formula  $p=m+1$ . As follows from our data, for the stratosphere  $p$  is equal to  $3.6\pm 0.5$ , and for the troposphere  $p=3.2\pm 0.4$ . These values of  $p$  are corresponding to

Kolmogorov spectrum with  $p=11/3$  in limits of measurement errors. The fluctuation frequency  $F$  is connected to scale of irregularities  $l$  by formula  $F=V/l$ , where  $V$  is complete velocity of crossing of the irregular media by radio occultation ray. In analyzed events the velocity  $V$  changed in interval  $1.9 \dots 2.6 \text{ km}^{-1}$ . Thus the scales interval  $l \approx 0.6 \div 0.8 \text{ km}$  is corresponding to the fluctuation frequency  $F=3 \text{ Hz}$ .

## 2.2 Amplitude fluctuations at $\lambda=2 \text{ cm}$ (MIR/GEO experiment)

The presence in the stratosphere irregularities, different from classical Kolmogorov turbulence, stimulates interest to research in this area of the atmosphere. The stratosphere has stable stratification, suppressing vertical movements; this is a cause for formation anisotropic, extended along a horizontal direction, irregularities of density. Kan, Matyugov and Yakovlev, 2002, considered an opportunity of determination of parameters corresponding to isotropic and anisotropic irregularities in the stratosphere. They used a spectral analysis of amplitude fluctuations of centimeter radio waves observed during MIR/GEO radio occultation experiments.

Radio occultation ray crosses anisotropic irregularities, basically, in a vertical direction. In this case the frequency of amplitude fluctuations is determined by vertical component of velocity of a point C (Fig. 2.1). During inclined radio occultations the point C has a horizontal component of velocity  $V_h$ , which is perpendicular to plane of Fig. 2.1. We shall designate  $\alpha$  the angle of inclination,  $\alpha = \tan(V_h/V_B)$ . Spectral density at low frequencies grows with increasing  $\alpha$ , because the frequencies of amplitude fluctuations caused by influence of anisotropic irregularities are displaced to low-frequency domain owing to reduction of  $V_B$ , opposite to increasing of the complete velocity  $V$ , connected with relative movement of the satellites. In the case of isotropic irregularities, on the contrary, the frequencies of fluctuations grow with increasing of velocity  $V$  and, accordingly, spectral amplitudes in low-frequency domain decrease. Thus, separation of the spectra of amplitude fluctuations corresponding to isotropic and anisotropic turbulence components may be observed when  $\alpha$  is increasing. Therefore the measurements should be carried out at the condition when appreciable frequency separation of the contributions of anisotropic and isotropic irregularities is observed in spectral density of fluctuations. Separation in frequency domain allows more precise estimation of inclinations in high-frequency domain owing to smaller mutual covering of spectra, caused by isotropic and anisotropic irregularities. Kan, Matyugov and Yakovlev [2002] carried out analysis of an opportunity of monitoring of the statistical characteristics stochastic irregularities of density and temperature of stratosphere using data of amplitude measurements and compared results of radio occultation experiments, carried out in centimeter range of radio waves, with the theory. In Fig. 2.6 experimental and theoretical frequency spectra of amplitude fluctuations in height interval from 36 up to 18 km are shown for radio occultation event May 26, 1998, corresponding to region with coordinates  $40.5^\circ(\text{N}$  and  $62.2^\circ \text{ E}$ . Average magnitude of the height  $h$  and root-mean-square value of amplitude fluctuations  $\sigma_E$  are specified near the appropriate spectrum. On vertical axes on Fig. 2.6 values of dimensionless function  $fG_E$  are indicated, on horizontal axes – the frequency of fluctuations  $f$  is shown. The experimental values  $fG_E$  are shown in Fig. 2.6 by triangular badges. The thin broken lines, designated by number 1 (upper left figure), show spectral density of noise measured in the free space. The theoretical spectra, calculated for isotropic Kolmogorov turbulence, are indicated by dotted curves, designated in Fig. 3 only for spectra at the upper left. Spectra, corresponding to strong anisotropic irregularities, which

has been calculated by means of appropriate model of saturated internal gravitational waves, are shown by curves 2. Assuming regime of weak fluctuations, and statistical independence of the isotropic and anisotropic irregularities, their common contribution may be considered as a sum of spectra for each type of irregularities. The total theoretical spectrum of amplitude fluctuations is shown in Fig. 2.6 by thick line, designated by number 4. Curves 2 coincide with curves 4 up to frequency  $f \approx 10$  Hz.

At angles realized in MIR/GEO radio occultation experiments the diffraction maxima of theoretical spectra for anisotropic irregularities corresponded to frequencies 3.5...4 Hz, and for isotropic irregularities – 13...13.5 Hz. Strong separation of spectra in frequency domain facilitates their selection. It is visible from Fig. 2.6, that amplitude fluctuations of a radio signal in the stratosphere, basically, are determined by influence of anisotropic irregularities. Anisotropic irregularities introduce main contribution in dispersion of amplitude fluctuations. The contribution of Kolmogorov turbulence in amplitude fluctuations is small. The contributions isotropic and anisotropic irregularities are comparable only in frequency interval  $f > 10$  Hz, in the domain of recession of experimental spectra, where influence of noise is essential. In the troposphere the ratio of contributions of isotropic and anisotropic turbulence may different than in the stratosphere, the amplitude fluctuations corresponding to Kolmogorov turbulence are expressed much stronger.

### Figures

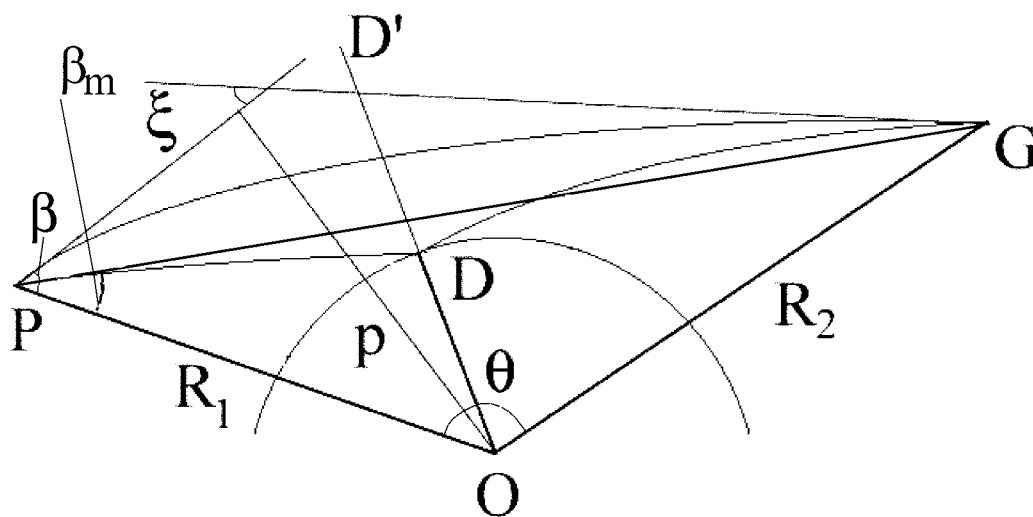


**Fig. 1.1:** Scheme of radio occultation at  $\lambda = 19$  and 24 cm (GPS/MET experiments) and  $\lambda = 2$  and 32 cm (MIR-GEO experiments)

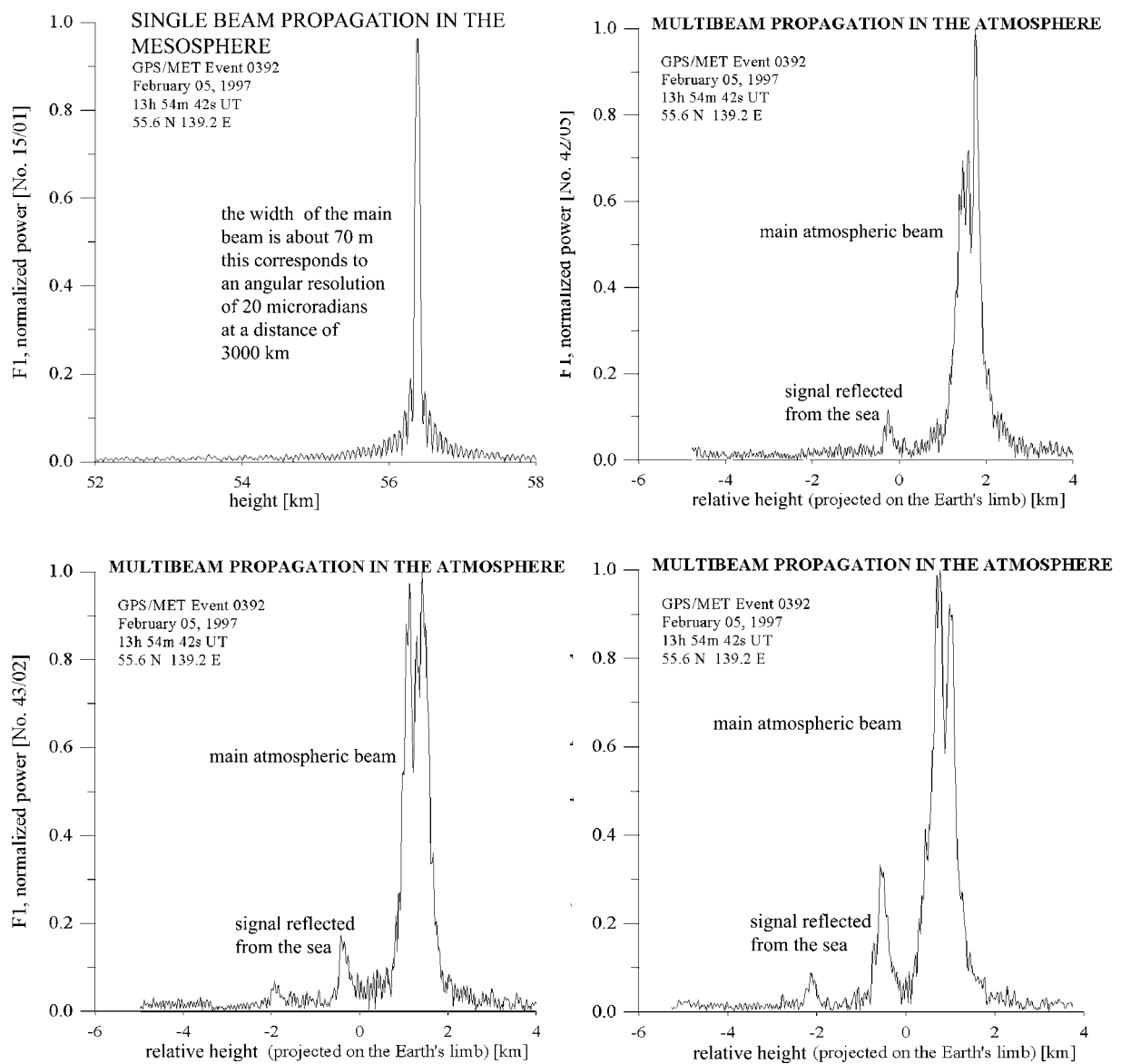


**Fig. 1.2:** Radio brightness distribution in the Earth’s atmosphere as seen from the LEO satellite. Top left panel: mesosphere, single beam propagation, a vertical resolution of about 70 m. Top right and two lower panels: the signal, that has been reflected from the sea, is very well resolved relative to the main beam in the troposphere. The time interval between successive plots is about 0.48 seconds. Comparing the position of the reflected signal in neighboring panels shows the motion of the main beam.



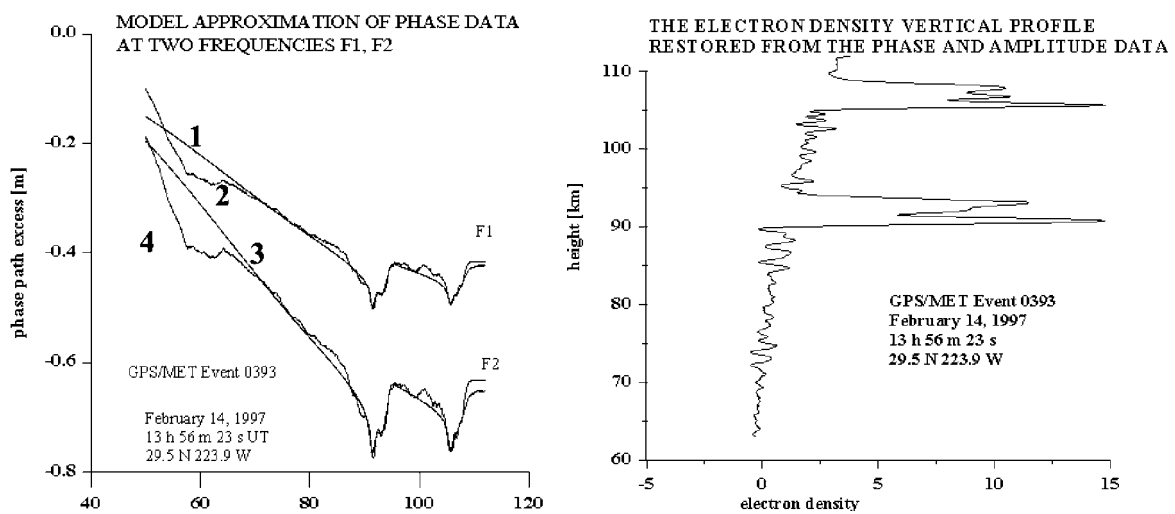


**Fig.1.3:** Comparison of the phase of reference beam (curves 1 and 3 in the left panel) as function of the height with radio occultation phase excess data at frequencies F1=1575.42 MHz and F2=1227.6 MHz (curves 2 and 4 in the left panel). The result of restoration of the vertical electron density distribution  $N_e \cdot 10^{-9} [1/m^3]$  from using radio holography approach (right panel).

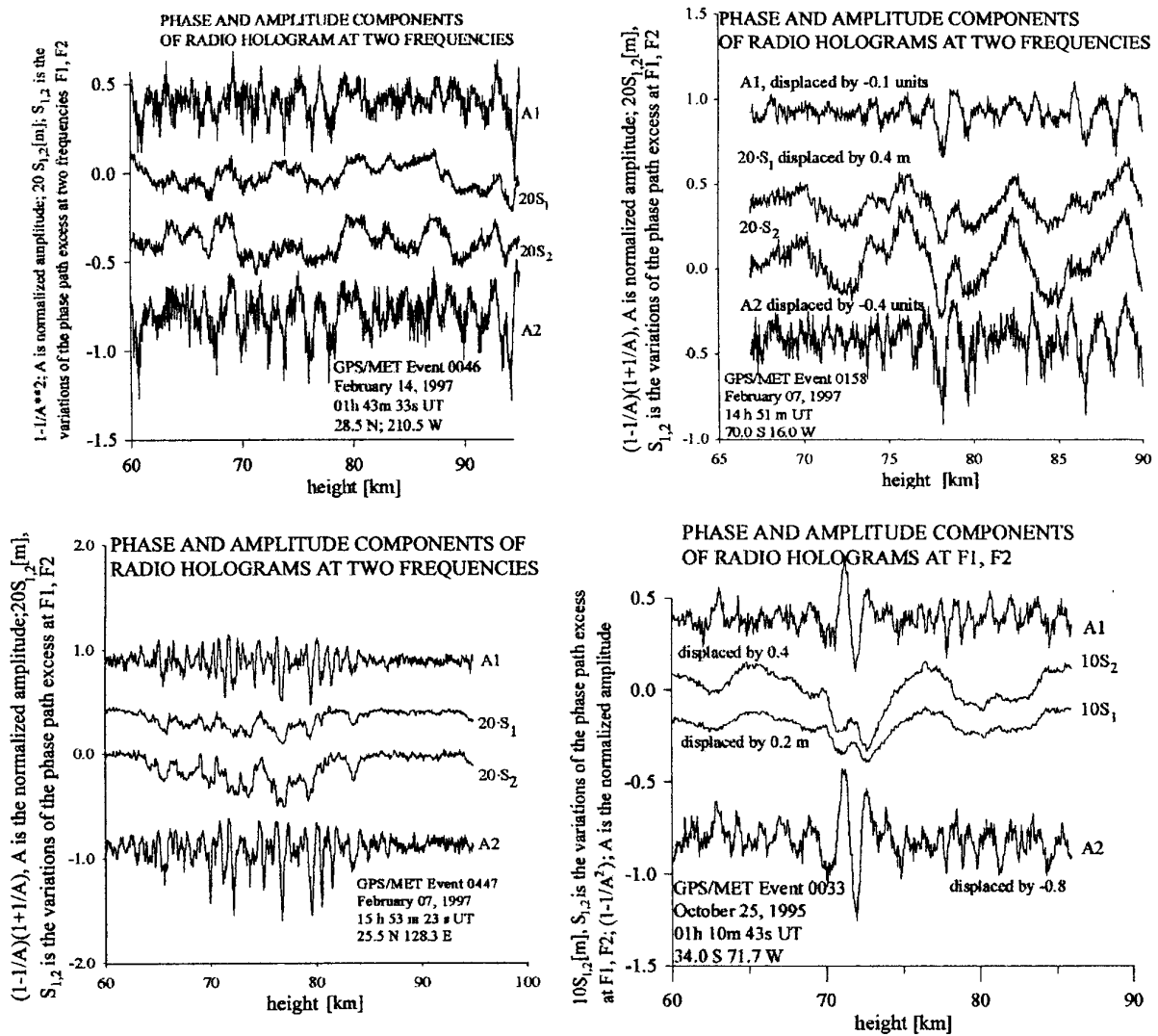
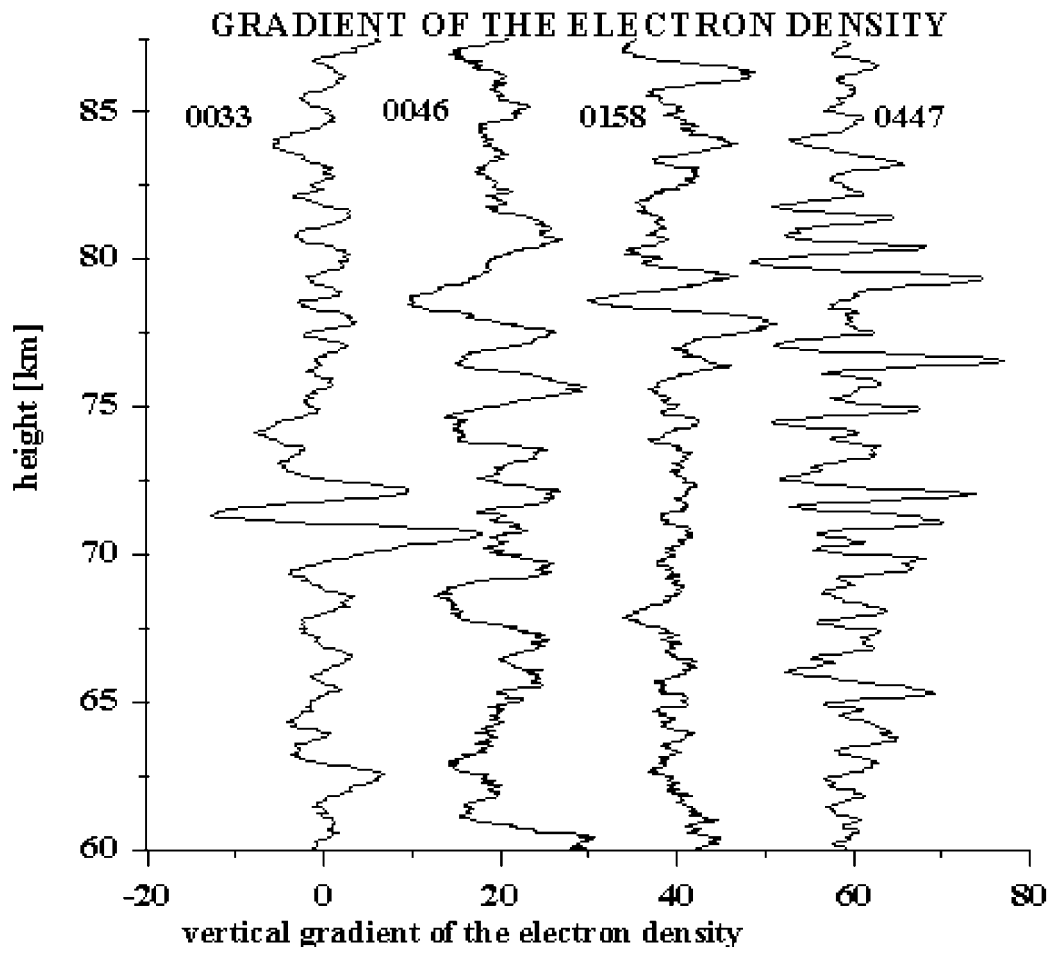


Fig. 1.4: Radio holograms of the D-layer of the ionosphere.



**Fig. 1.5:** Vertical gradient of the electron density altitude distribution  $dN_e/dh \cdot 10^{-9} [1/m^3 km]$

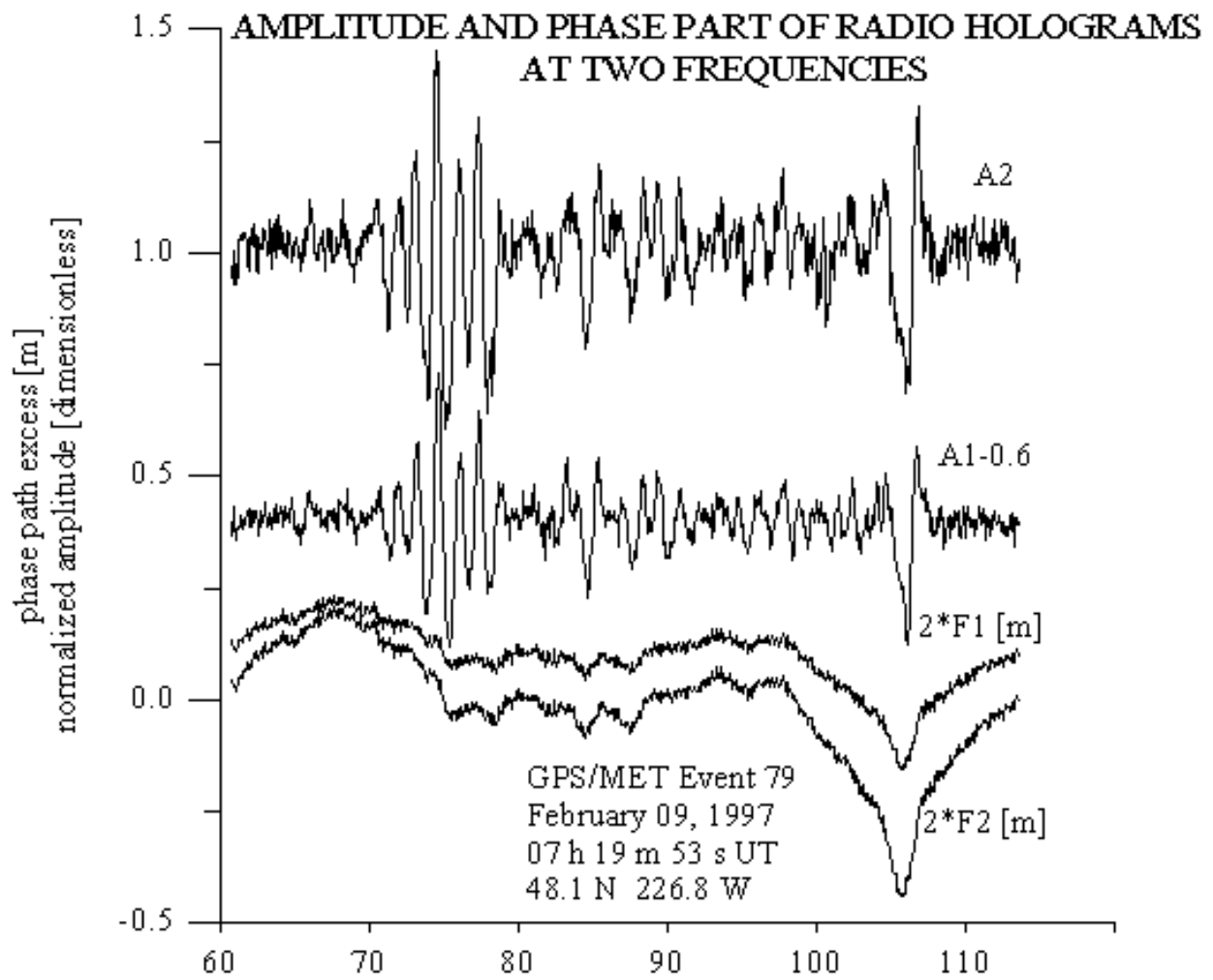
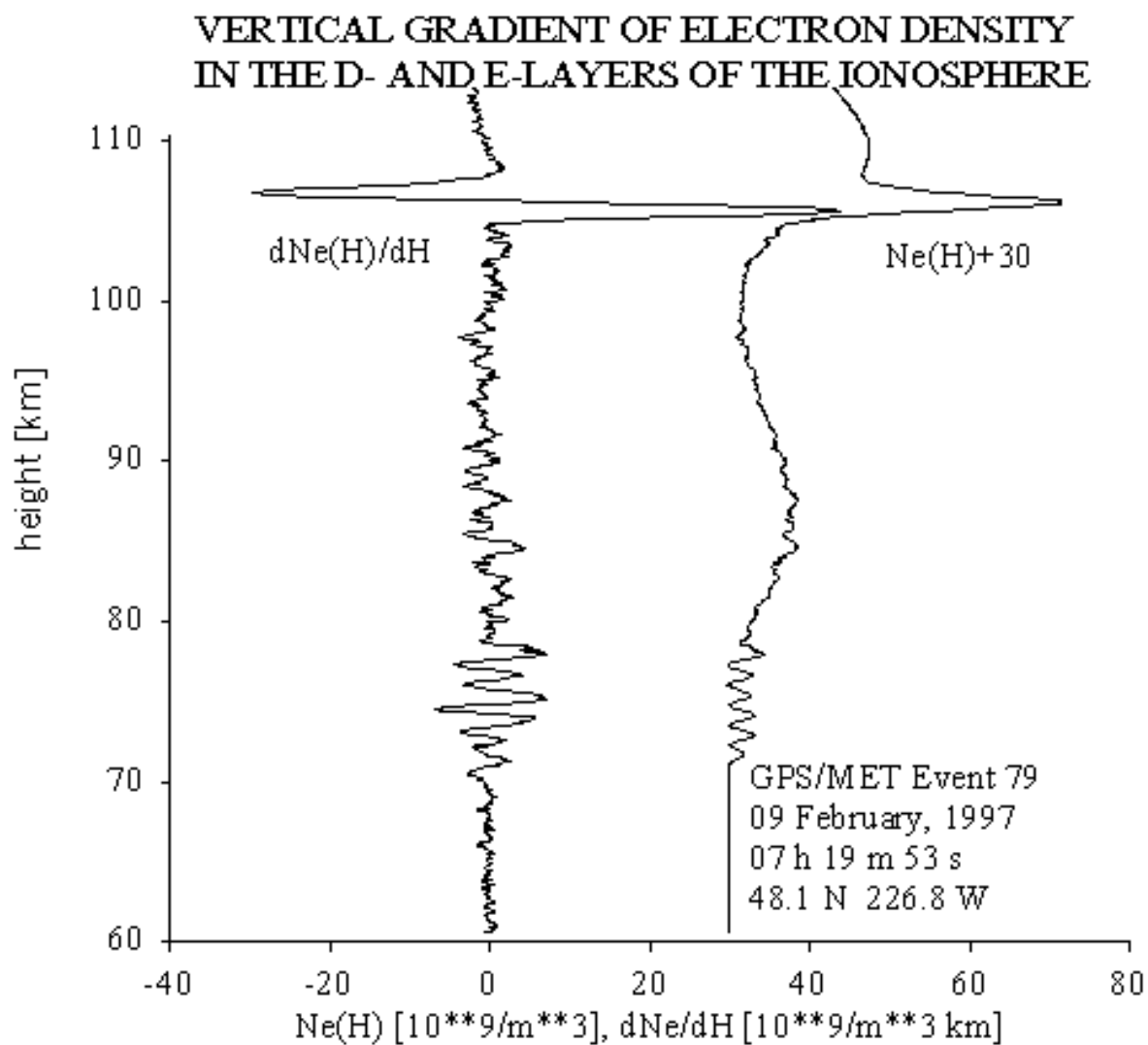


Fig. 1.6: Comparing phase and amplitude data at two frequencies.



**Fig. 1.7:** Sporadic E-layer (height interval 105-108 km) and zone of internal wave breaking in the D-layer (heights 70-78 km) in the lower ionosphere (near local midnight) as seen from radio holography analysis of GPS/MET radio occultation data.

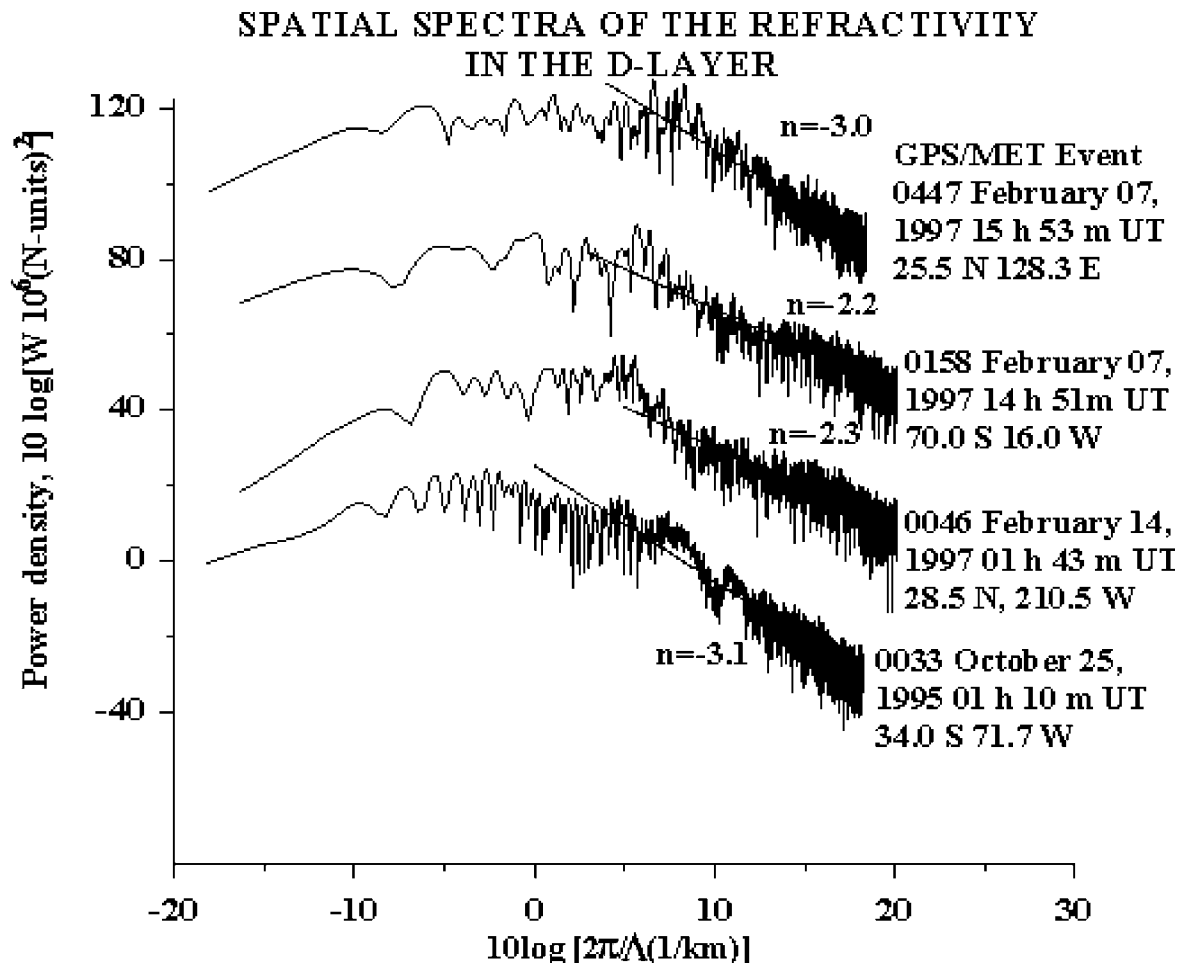
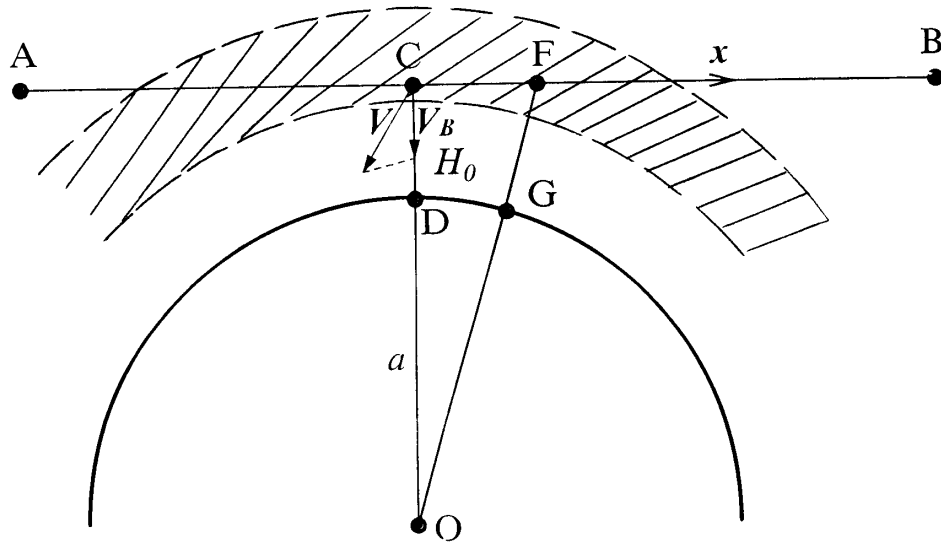
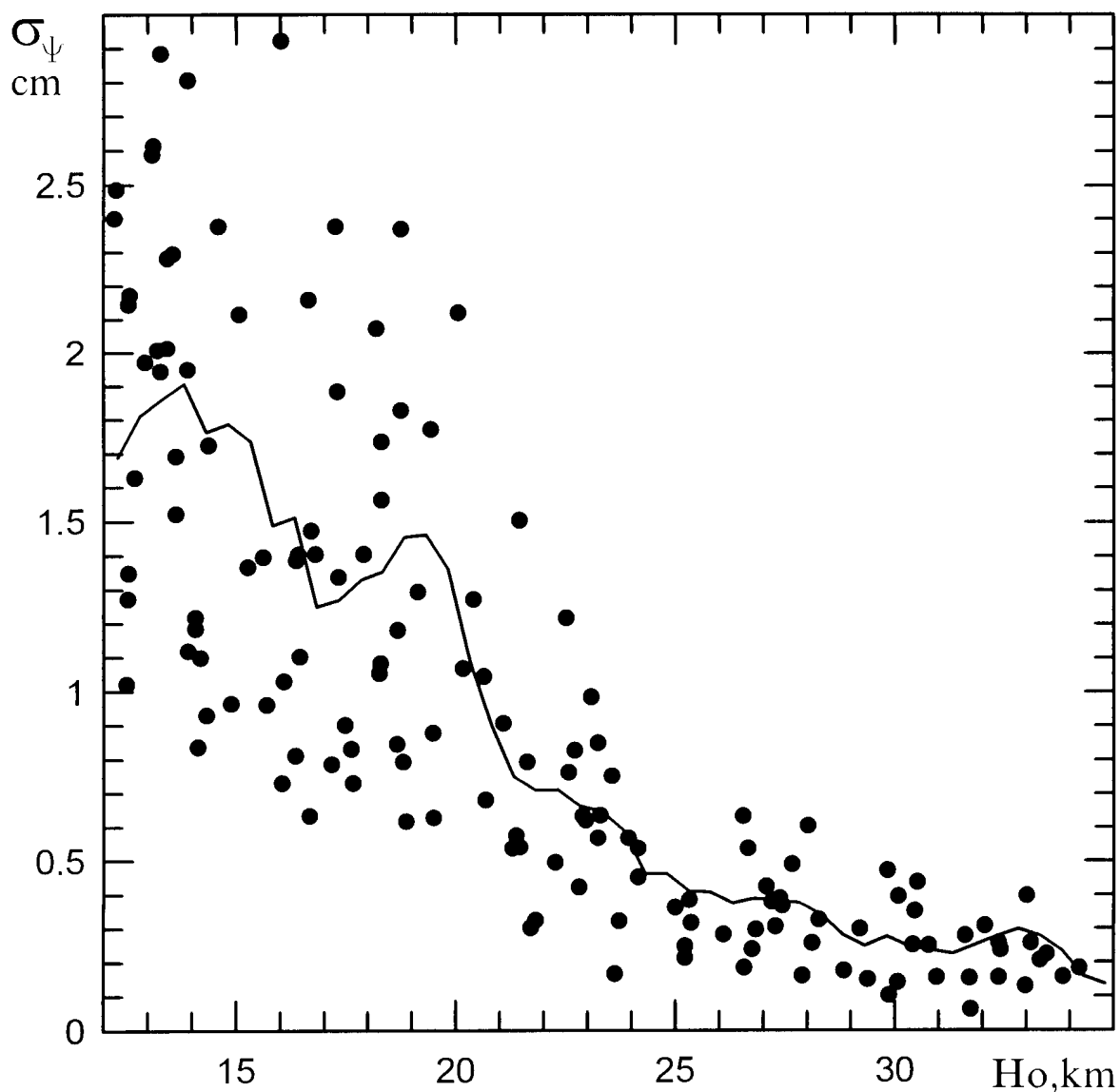


Fig. 1.8: Spatial spectra of waves in the D-layer of the ionosphere.



**Fig. 2.1:** Scheme of sounding of ionospheric (shaded) and atmospheric irregularities.



**Fig. 2.2:** RMS of phase fluctuations in the stratosphere plotted against the minimum ray height  $H_0$ . Points show experimental data. Solid curve shows result of averaging.



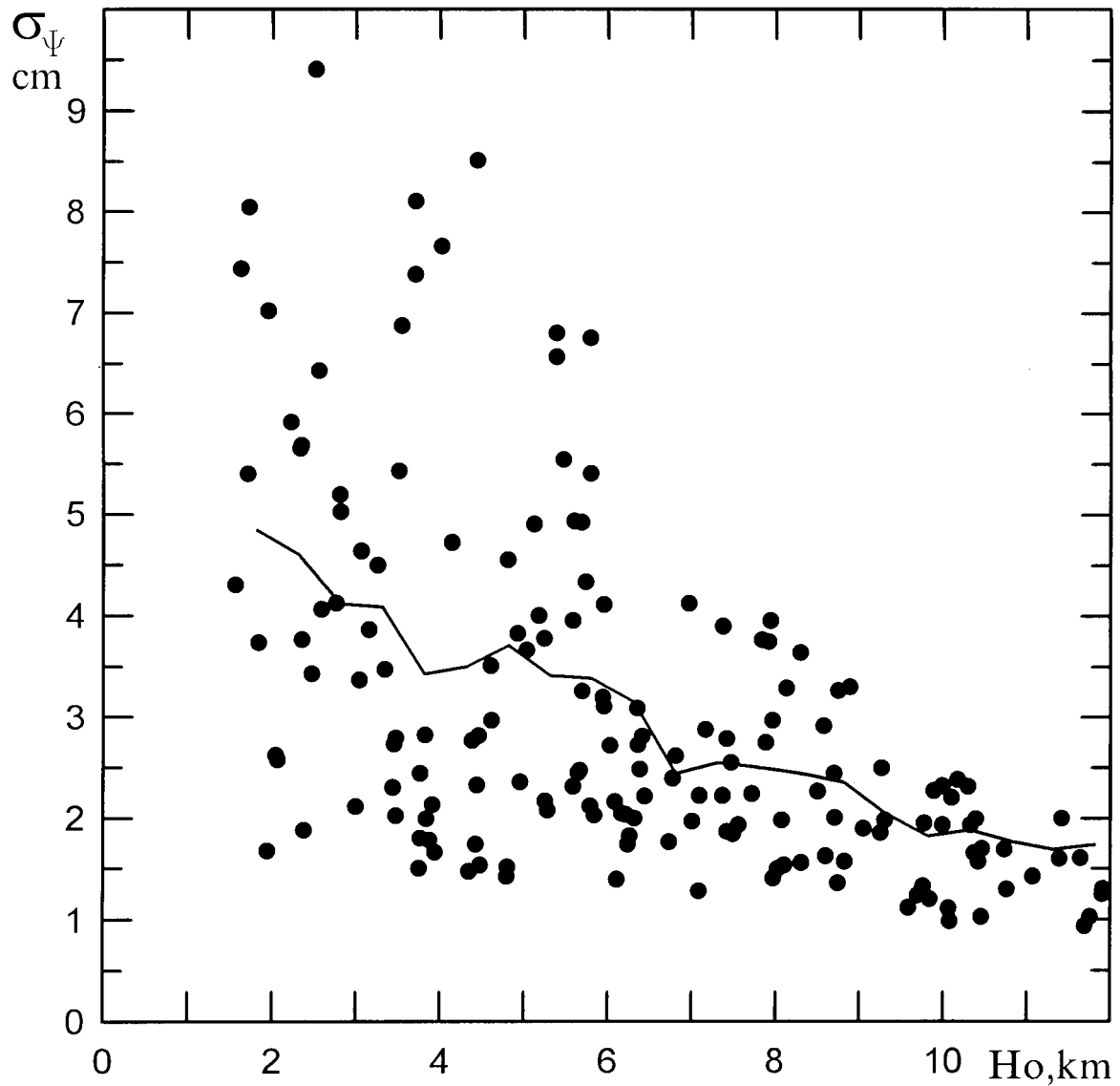


**Fig. 2.3:** RMS of phase fluctuations in the troposphere plotted against the minimum ray height  $H_0$ . Points correspond to experimental data. Solid curve shows result of averaging.

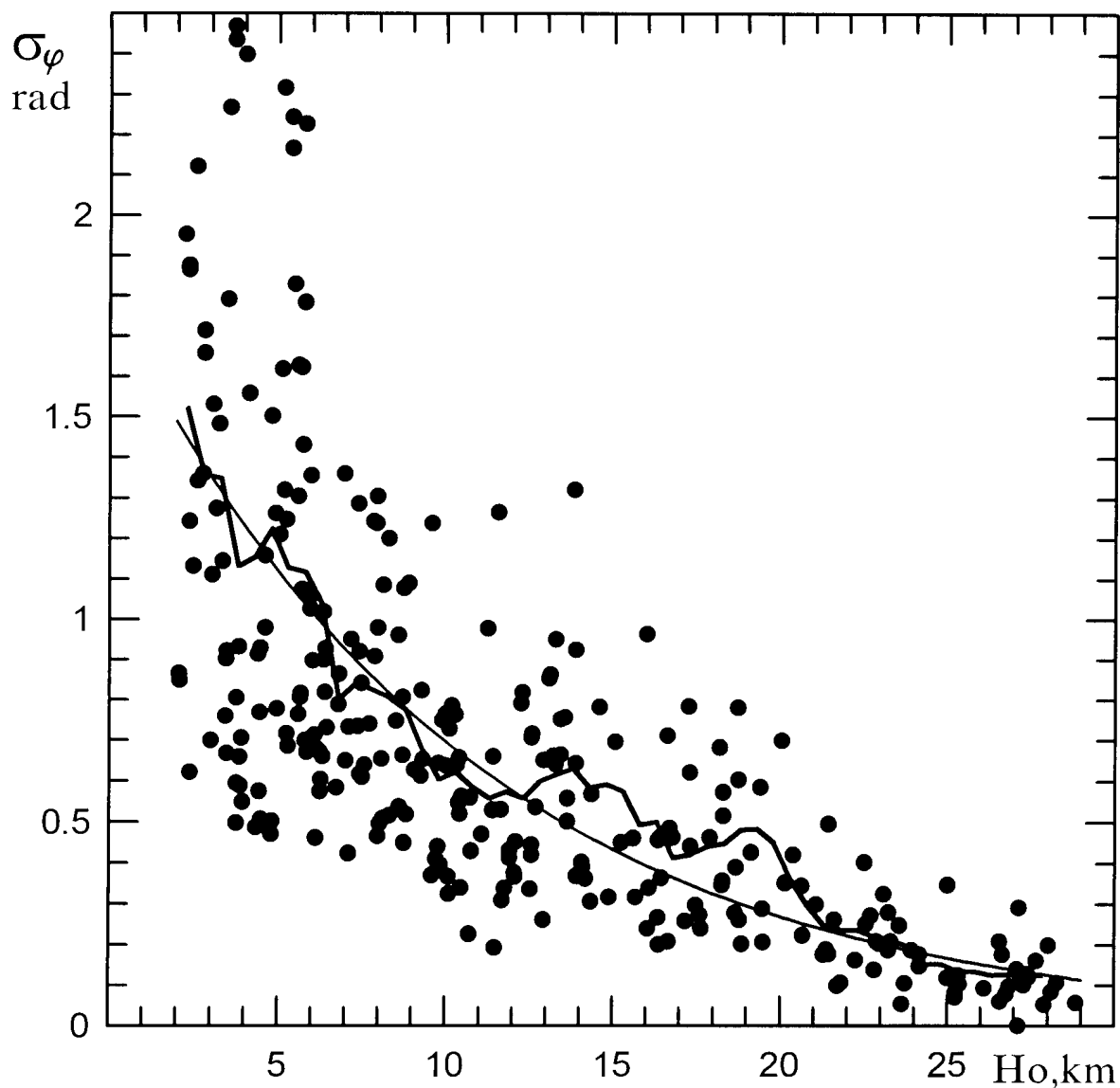


**Fig.2.4:** RMS of phase fluctuations plotted against the minimum ray height  $H_0$ . Points correspond to experimental data. Broken solid curve shows result of averaging and smooth curve corresponds to model of dependence  $\sigma_\varphi(H_0)$ .

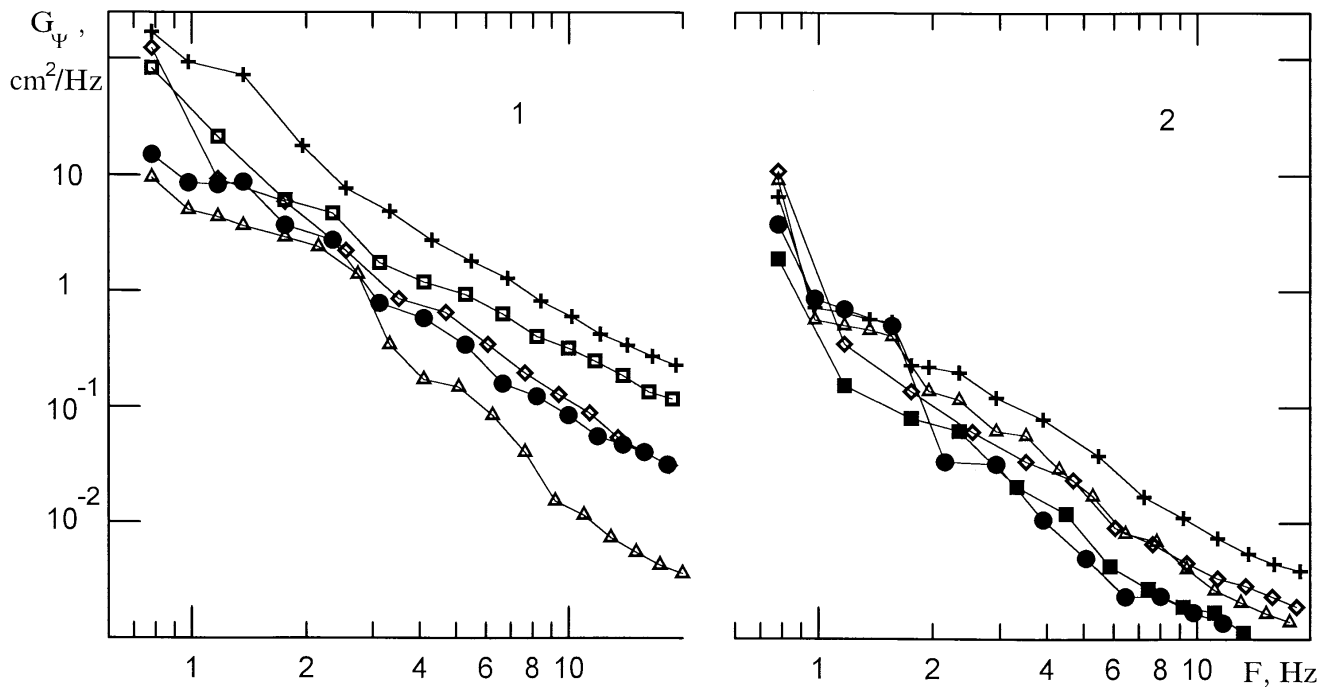


**Fig. 2.5:** Typical spectra of phase fluctuations in the troposphere (1) and in the stratosphere (2).

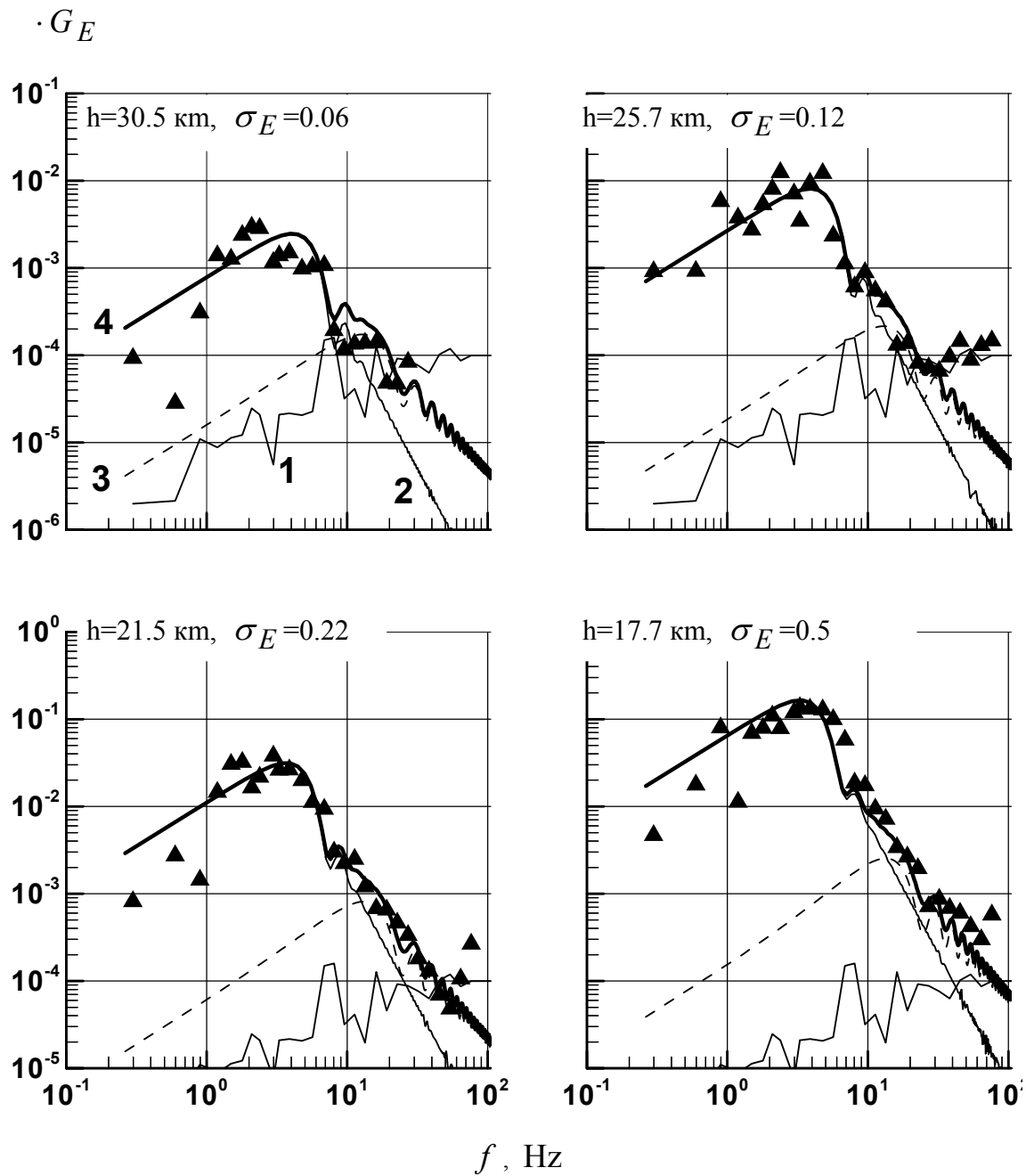


**Fig. 2.6:** Spectra of amplitude fluctuations corresponding to isotropic (Kolmogorov's type, curve 3 in the upper left panel, and dotted lines in the upper right and lower panels), and anisotropic turbulence (triangles-experimental data, thick curve 4 shows resulting spectra describing joint effect of isotropic and anisotropic turbulence) as measured in MIR/GEO radio occultation experiments. The curve 2 shows spectra corresponding to anisotropic turbulence. The noise spectra is indicated by curve 1 in the upper left panel and by breaking lines in the upper right and lower panels.

## Summary

This report contains description of the results obtained in IRE RAS during the sixth stage of works owing to calendar plan of joint investigations with GeoForschungsZentrum Potsdam (GFZ-Potsdam). The plan of work that must be fulfilled in IRE RAS during the sixth stage consists in description main results of radio holographic method for delivering recommendation for its application for analysis radio occultation data. In the first section of this report the main features of radio holographic method is considered. Generalization of radio holographic method for three-dimensional (3-D) case is proposed. This generalization may be applied in future for developing polarization radio holography with aim of monitoring polarization-sensitive natural objects (rains, snow clouds etc.) in the Earth's atmosphere using signals, emitted by navigational and telecommunication satellites. It is shown that radio holographic method is a generalized form of backward propagation method. Radio holographic method in the proposed form may obtain, simultaneously, high vertical resolution and accuracy in estimation of the refraction angle and impact parameter. The effectiveness of radio holographic method was shown by means of revealing reflected signals in the GPS/MET and CHAMP radio occultation data. Combined radio holographic analysis of the phase and amplitude data allows observations of wave structures in the upper atmosphere and accurate measurements of the altitude profiles of the electron density and its vertical gradients in the D- and E- layers of the ionosphere. In the second part the results of measurements of turbulence parameters in the atmosphere is considered. Nowadays radio occultation method is applied basically for analysis of regular structures including information on altitudes profiles of the density, temperature, pressure and humidity in the atmosphere and electron density in the ionosphere. However radio occultation method allows recovering information on the statistical properties of the atmospheric and ionospheric irregularities, which are connected with turbulence and wave processes. Information on the statistical irregularities is important for study processes of energy changes between the upper and lower atmosphere. Investigations in this direction are now in the early stage of development. In the second part of the report the preliminary results are given describing elaboration of radio occultation method for determination of turbulence and wave structures in the atmosphere. The final results obtained during investigations provided in 2001 year in frame of GFZ/IRE contract are:

1. Generalization of radio holographic method for 3-dimensional case and inhomogeneous media is presented. The 3-dimensional form of radioholographic method accounts for polarization of electromagnetic waves and may be used in future for elaborating new direction of investigation: polarization radio holography for recovering polarization-sensitive objects in the atmosphere and ionosphere.
2. It is shown that 2-D focused synthetic aperture radioholographic method derived early by *Pavelyev [1998]*, *Hocke et al. [1999]*, *Igarashi et al. [2000]* gives full solution of the task of the backward propagation approach and gives vertical resolution about of 60...80 m as follows from analysis of radio occultation data. For achieving extreme vertical resolution about of 1/20...1/100 of the size of Fresnel zone it is necessary to construct new radio holographic algorithms. These algorithms will use effective processes of solution of direct and inverse refraction and diffraction problem for inhomogeneous media and must work in real time. Developing new practical procedures of radio holographic analysis of radio occultation data is a task for future investigation.

3. Validation of 2-D focused synthetic aperture radiographic method is fulfilled by means of discovering reflected signals in GPS/MET data and measuring parameters of wave structures in the upper atmosphere. Radio images of the atmosphere and terrestrial surface are obtained using GPS/MET radio occultation data. Radio images may be used for bistatic scatterometry of the terrestrial surface: determination parameters of the sea surface (for example, estimation of heights and slopes of the wind roughness) and land. Radio images of the atmosphere may be used for estimating parameters of multibeam propagation and vertical profiles of the refractivity, temperature and humidity in the boundary layer. Model describing dependence of the phase path, amplitude and frequency of reflected signal on vertical profile of the refractive index and absorption in the atmosphere is developed. This model may be used in future for measurements of the refractivity and absorption in the boundary layer of the atmosphere.

4. It is shown that combined analysis of phase and amplitude information contained in the radiograms at two frequencies reveals altitude profiles of the vertical gradients of the refractive index in the upper atmosphere. Derived algorithms may be used for recovering atmospheric and stratospheric wave structures and temperature gradients.

5. Ionospheric correction algorithm is developed. This algorithm excluded influence of the upper layer of the F-layer for quiet condition in the ionosphere. Influence of the ionosphere may be considered as a slow trend, which may be subtracted from the phase data at two frequencies. It is shown that for quiet ionospheric conditions influence of layered structures near turning point of a radio occultation ray is about of 40 dB greater than effect of upper ionosphere irregularities on radio occultation signal. In the case of high solar activity the influence of the upper ionosphere may be essential especially near auroral oval and near geomagnetic equator. In this case amplitude and phase fluctuations of the radio occultation signal caused by the upper ionosphere may be higher than effects of layered structures in the atmosphere and lower ionosphere. Excluding of the ionospheric effect in the case of high solar activity is the subject of future work.

6. The possibility of monitoring of the density and temperature fluctuations in the stratosphere from radio occultation amplitude measurements in centimeter band for satellite-to-satellite links has been analyzed. The comparison of the experimental spectra of amplitude fluctuations with the theoretical spectra, calculated for model containing both strongly anisotropic irregularities and isotropic Kolmogorov's turbulence showed that a basic contribution is carried in the stratospheric amplitude fluctuations by the anisotropic irregularities, which correspond to model of the saturate internal gravity waves. The efficacy of the radio occultation technique for the global remote monitoring of the internal stratospheric waves has been shown.

## **Recommendations**

Radioholographic method opens new perspectives for radio occultation investigations of the atmosphere, ionosphere and terrestrial surface using signals of navigational, broadcast- and-TV satellites on the telecommunication line satellite-to-satellite. So it is necessary to prolong work on radioholographic analysis of existing data base of radio occultation events (GPS/MET, CHAMP) in mass scale to obtain new precise information on natural processes in the atmosphere, mesosphere and on the Earth surface. Internal waves in the atmosphere and mesosphere may be recovered in the temperature and electron density vertical gradients measured by radio holographic method. Especially interesting are looking for simultaneous measurements of wave structures in the D- and E-layers and sporadic E-layer with observations of the Earth-based ionosondes.

Observations of the internal waves activity are important for estimation of intensity of the atmospheric processes in different regions of the Earth. It is important to develop new algorithms for measurements of parameters of the boundary layer of the atmosphere by means of simultaneous observations of direct and reflected signals. The temperature and humidity distribution in the boundary layer contains information on heat transfer between the surface and atmosphere. The new methods are necessary for separating of the effects of turbulence and regular structures in radio occultation signal because turbulent layers correspond to regions with maximum heat exchange in the atmosphere. Radio holographic method is appropriate for solution of these tasks because its accuracy and vertical resolution corresponds to high-precision level of radio navigational satellites. Special interest consists in radio holographic analysis of experimental data obtained during MIR/GEO radio occultation experiments at wavelength 2 cm. Radio occultation data obtained in centimeter wave band are more sensitive to details in the vertical distribution of the humidity, temperature and absorption. Their analysis is recommended for derivation new methodology for planned radio occultation missions.

## References

- Dalaudier, F., A.S. Gurvich, V. Kan, and C. Sidi, Middle stratosphere temperature spectra observed with stellar scintillation and in situ techniques. *Adv. Space Res.*, v. 14, N 9, p. 61-64, 1994.
- Gorbunov, M.E., S.V. Sokolovskii, and L. Bengtsson Space Refractive Tomography of the Atmosphere: Modelling of Direct and Inverse Problems *Paper 210* Max-Planck-Institute for Meteorology ISSN 0937-1060, 1996.
- Gorbunov, M.E., A.S. Gurvich, and L. Kornbluh, Comparative analysis of radio holographic methods of radio occultation data. *Radio Science*, **35**(4), 1025-1034, 2000.
- Gurvich, A.S. and V. Kan, Radio wave fluctuations in satellite-atmosphere-satellite links: Estimates from stellar scintillation observations and their comparison with experimental data (in Russian). *Izv. Akad. Nauk, Fiz. Atmos. i Okeana*, v. 33, N 3, p. 314-323, 1997.
- Hocke, K., A. Pavelyev, O. Yakovlev, L. Barthes and N. Jakowski, Radio occultation data analysis by radio holographic method. *JASTP*, **61**, 1169-1177, 1999.
- Igarashi, K., A. Pavelyev, K. Hocke, D. Pavelyev, and J. Wickert, Observation of wave structures in the upper atmosphere by means of radio holographic analysis of the radio occultation data. *Advances in Space Research*, **27**, No. 6-7, 1321-1327, 2001.
- Igarashi, K., A. Pavelyev, K. Hocke, D. Pavelyev, I.A. Kucherjavenkov, S. Matugov, Zakharov, and O. Yakovlev. Radio holographic principle for observing natural processes in the atmosphere and retrieving meteorological parameters from radio occultation data. *Earth Planets Space*, **52**, 968-875, 2000.
- Ishimaru, A., *Wave Propagation and Scattering in Random Media*, Academic Press., v. 2, 1978.
- Kan, V., S.S. Matyugov and O.I. Yakovlev, Structure of stratospheric irregularities from radio occultation data on satellite-to-satellite links. Accepted for *Izv. Vuz-ov. adio Fizika*, 2002, (in Russian).
- Karayel, E.T. and D.P. Hinson, Sub-Fresnel-scale vertical resolution in atmospheric profiles from radio occultation. *Radio science*, **32**, No.2, P.411-428, 1997.
- Mortensen, M.D., R.P. Linfield and E.R. Kursinski. Vertical resolution approaching 100 m for GPS occultation of the Earth's atmosphere, *Radio Sci.*, **34**, No.6, 1475-1484, 1999.
- Pavelyev, A., On the possibility of radio holographic investigation on communication link satellite-to-satellite. *Radiotekhnika i elektronika* **43**, No. 8, 939-944, 1998 (in Russian).
- Pavelyev A. Statement of radio holographic problem, in Report 4 "Improvement of radio holographic method by using of reflected signals" GASP/IRE-2, fourth stage July-August 2001.
- Pavelyev A.G., O.I. Yakovlev, S.S. Matyugov, D.A. Pavelyev, and V.A. Anufriev, Advanced Algorithms of Inversion of GPS Radio Limb Sounding Data. Institute of Radio Engineering and Electronics of Russian Academy of Sciences. *Final Report, N 1-00*, 2000.



- Tsuda T., T. Van Zandt, M. Mizumoto, S. Kato, and S. Fukao. Spectral analysis of temperature and Brunt-Vaisala frequency fluctuations observed by radiosondes. *J. Geophys. Res.* **96** (D9), 17,265-17,278, 1991.
- Stratton J. W. *Electromagnetic Theory* Ed. McGraw-Hill Book Company, Inc. New York and London, 616 p., 1941.
- Smith, S.A., D.C. Fritts, and T.E. Van Zandt, Evidence for a saturated spectrum of atmospheric gravity waves. *J. Atmos. Sci.*, v. 44, N 10, p. 1404-1410, 1987.
- Vilkov I.A., S.S. Matyugov, and O.I. Yakovlev, Amplitude fluctuations in radio occultation data due to influence of the Earth's atmosphere. *Radiotekhnika and Elektronika*. V. 38, No. 5, 795-803, 1993. (in Russian).
- Wehner, D. R. *High Resolution Radar*. Ed. Artech House, inc. 685 Canton Street Norwood, MA 02062, 1987. International Standard Book Number: 0-89006-194-7. Library of Congress Catalog Card Number: 8-931.
- Yakovlev O.I., Pavelyev A., S.S. Matyugov, D. Pavelyev, V.A. Anufriev Advanced algorithms of inversion of GPS radio limb sounding data. Scientific Technical Report STR01/06. Part 3. Ionospheric correction and revealing ionospheric features. pp.52-72. 2001. GeoForschungsZentrum Potsdam.
- Yakovlev, O.I, S.S. Matyugov, I.A. VilkovA., et al., Radio-Wave Phase and Frequency Fluctuations as Observed in Radio occultation experiments on the satellite-to-satellite link. *J. Commun. Technology. and Electronics*, v. 41, N 11, p. 993-998, 1996.